UNIVERSITY OF CRAIOVA
ELECTRICAL ENGINEERING FACULTY

M.Sc. Alin-Iulian DOLAN

ABSTRACT OF PHD. THESIS

Contributions to modeling of the fields and of the transient regimes in electrical equipments

Scientific coordinator:
Prof. Grigore A. CIVIDJIAN

CRAIOVA, 2009

ACKNOWLEDGEMENTS

I owe my deepest gratitude to scientific coordinator, Prof. Grigore A. Cividjian, for very meticulous guidance, scientific advices and critical comments, extremely valuable in accomplishing this work.

I'm honored by and I thank to Prof. Andrei Țugulea, member of Romanian Academy, to Prof. Mihai Iordache, Prof. Dumitru Topan and Prof. Ioan Popa, for accepting to make the peer review of the thesis.

Thank once again to Prof. Dumitru Topan and to Prof. Ioan Popa, for the encouragements given at the appropriate time for undertaking steps in obtaining abroad internships, which have enriched my scientific and linguistic horizon.

Also thank to the University Agency for Francophonie, for the financial support to achieve the inter-university mobility and to Prof. Serge Monchaud from the National Institute of Applied Sciences in Rennes, for the careful coordination of its beginning in the Technical University of Sofia.

Thank to the French Institute in Sofia, for its hospitality and special support in rapid assimilation of the French language.

I want to thank Prof. Ivan Yatchev from Technical University of Sofia, for his great hospitality and assistance in using the ANSYS *program, along the research internships undertaken at the Doctoral School from this university, making possible the extension of the numerical simulations related to Chapters III and IV.*

Thank, by this way, to Prof. Leonardo-Geo Mănescu, for kindly helped to me in contacting the professors and specialists from Grenoble Electrical Engineering Laboratory, referring Prof. Gérard Meunier, Prof. Albert Foggia and Prof. Thierry Chevalier, whom I thank for their hospitality and support in using the FLUX *program, along the research internship undertaken at this laboratory.*

In the same time I thank to CEDRAT *Company in Grenoble for the rights of personal use of the* FLUX *program, which had allowed the numerical simulation related to the chapters V and VI.*

I want to thank all colleagues in the Department of Electrical apparatus and technologies, for many encouragements and very useful advices along this work.

I thank and am deeply grateful to my family for the moral support, the understanding and patience, constantly exhibited, helping me to finalize this thesis.

SUMMARY

Abbreviations list

AN – analytic solution;
ANSYS – 2-D and 3-D FEM modeling software;
APLD – ANSYS Parameter Design Language, used by ANSYS program;
ATP-EMTP – Alternative Transients Program - Electromagnetic Transients Program, modeling power systems components package;
NE – nodal elements;
EE – edge elements;
FEMM – Finite Element Method Magnetics, 2-D FEM modeling software;
FLUX – 2-D and 3-D FEM modeling software;
IPTM – DELPHI application for internal inductance determination of a plunger-type electromagnet;
LUA – parameter language, used by FEMM;
PABCM – power approximation of boundary conditions method;
EMCM – equivalent magnetization current method;
FDM – finite differences method;
FEM – finite element method;
BEM – boundary elements method;
VWM – virtual work method;
CVWM – Coulomb virtual work method;
ESM – equivalent sources method;
EMCM – equivalent magnetic charges method;
FVM – finite volume method;
CMM – conformal mapping method;
MTM – Maxwell stress tensor method;
NUM – numerical solution;
ESP – electric scalar potential;
MSP – magnetic scalar potential;
MSPd – difference magnetic scalar potential;
MSPg – generalized magnetic scalar potential;
MSPe – edge magnetic scalar potential;
MSPr – reduced magnetic scalar potential;
MSPt – total magnetic scalar potential;
MVP – magnetic vector potential;
QUICKFIELD – 2-D FEM modeling software;
SC – Schwartz-Christoffel module of MATLAB program (numerical conformal mapping);
TPTLEC – transient parameters theory of linear electric circuits;
FVT – final value theorem;
IVT – initial value theorem;
2-D – two-dimensional;
3-D – three-dimensional.

INTRODUCTION

The paper contains contributions in numerical modeling of electric and magnetic fields, established in electrical equipments or their accessories in normal operating and unexpected or controlled transient regimes.

The basic tool used in all numerical simulations is the finite element method (FEM) for which the author has done thorough research both theoretically, concerning the variety of formulations developed over time and obtaining competences in the use of specialized programs, commercial or noncommercial, in which the method is implemented: QUICKFIELD, FEMM, ANSYS, FLUX.

The thesis aims to validate analytical formulas deduced in approximate hypotheses and numerical computation of electric or magnetic, local or global quantities, experimentally obtained. In some cases, combined analytical-numerically solutions were proposed.

The variety of formulations of the FEM applied to concrete problems and the extraction techniques of local or global quantities from numerical field solution led to obtaining parallel results allowing a comparison between formulations and techniques in term of numerical resources and required time to solve the problems, pointing out the effectiveness of some of them.

The thesis is structured into seven chapters, beginning with fundamental description of the projective and variational formulations (Chapter 1). Since the method has targeted magneto static applications, starting from customizing the electromagnetic field equations for this regime, were presented its various formulations, sustained by an extensive review of recent literature.

The following chapters are two applications of 2-D and 3-D FEM: to calculate the inductance of plunger-type electromagnets (Chapter 2) and the magnetic force developed by such equipment (Chapter 3). The description of techniques for determining the global forces from field solution enjoys special attention, focusing important conclusions from published works in recent years.

The leakage flux in magnetic circuits has been studied for a power multi-winding, under load adjustable, autotransformer, for which 2-D and 3-D numerical models were created, that allowed, with a good precision, the short-circuit reactance computation (Chapter 4). Optimization of solutions in 3-D numerical simulations were searched to reduce the solving time and to increase the accuracy. The study concludes by analyzing the behavior of autotransformer at the application of lightning surges, using FEMM and ATP-EMTP programs, aiming the over voltages level on the no load tappings of regulating winding.

Chapters 5 and 6 concern the transient phenomena taking place in a system of parallel solid rectangular bars supplied with step and ramp signals of current and voltage. The results of numerical simulation of electric and magnetic fields penetration were compared with some analytical and combined with them to improve the effects of simplifying assumptions (Chapter 5). The transient parameters of the bar system were numerically determined and some of them were derived from some others, based on analytical relationships established by the theory of linear electric circuits transient parameters, making comments on certain irregularities found (Chapter 6).

In the last chapter (Chapter 7) the author's original contributions and conclusions are pointed out, structured in the chapters in which they appear, indicating the perspectives of their application.

Chapter I

FINITE ELEMENT METHOD FORMULATIONS

1.2 Projective formulation

FEM is one of the methods of continuous problems solutions representation by approximations on discretized domains [77]. The general method for approximating the sought function $u(x)$ is its representation by the projection on a finite size subspace, whose base is defined by $N+1$ *basic functions* (*projection functions*, *shape functions*) $\Phi_i(x)$:

$$\boldsymbol{u}(\boldsymbol{x}) \approx \sum_{i=0}^{N} q_i \Phi_i(\boldsymbol{x}) \tag{1.3}$$

1.3 Variational formulation

Many physical problems allow solutions approximation methods based on minimizing of functional corresponding usually to a type of energy. These are called variational formulations [21], [52], [168].

1.4 Unknown functions approximation

The approximate solution is sought as a linear combination of known basic functions [145], usually polynomial, linear or quadratic, set to take nonzero values only around certain particular points (*interpolation points*).

1.5 Finite element method formulations in Magneto statics

The solutions of the field problems are generally obtained using potential functions [3]. The magnetic scalar potential (MSP) or the magnetic vector potential (MVP) are often used for magnetic field.

1.5.1 FEM in magnetic scalar potential formulation (MSP)

MSP is of great importance in solving the 3-D magneto static problems because of its low cost of numerical calculation comparing to MVP consisting of three components and also without uniqueness problems [52], [82], [114]. There are different formulations (strategies) for obtaining the solution: reduced magnetic scalar potential formulation (MSPr), total magnetic scalar potential formulation (MSPt), difference magnetic scalar potential formulation (MSPd), generalized magnetic scalar potential formulation (MSPg), edge magnetic scalar potential formulation (MSPe).

1.5.2 FEM in magnetic vector potential formulation (MVP)

MVP is used in almost all magnetic field problems in witch occur current densities. It is very popular for 2-D or axi-symmetric applications because in these cases has only one component, orthogonal to the plane of analysis. In 3-D, the calculation is tripled and uniqueness problems occur, making it less attractive than MSP.

1.5.3 FEM in edge element formulation (EE)

The classical formulations of FEM associate degrees of freedom to the nodes of the mesh, using nodal elements (NE). In another approach, the degrees of freedom associated to the elements edges, aiming determining the field line integral along them, based on edge elements (EE) [17]. Depending on the used potential and on the way of degrees of freedom association, there are different particular formulations: MSP-NE, MSP-EE, MVP-NE, MVP-EE.

Chapter II

INDUCTANCE OF PLUNGER-TYPE ELECTROMAGNET

2.1 Introduction

In the papers [32], [33], [35] is developing a new numerical method for power approximation of the boundary conditions (PABCM).

2.2 Power approximation of boundary conditions method (PABCM)

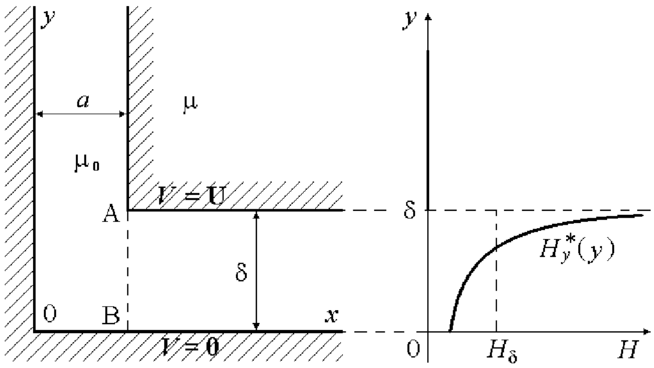

Fig. 2.1 - *Illustration of power approximation of boundary conditions method*

Analyzing the field in the vicinity of peak A with conformal mapping method, in the papers [32] and [33] is proposed to approximate tangential component of the magnetic field along the border AB, by the relationship (2.1), respecting the potential difference *U* (electric or magnetic) between A and B:

$$H_y^*(y) = H_\delta \left[k_1 + \frac{k_2}{\left(1 - \frac{y}{\delta}\right)^\alpha} \right], \; H_\delta = \frac{U}{\delta}, \; \alpha < 1, \; \int_0^\delta H_y^*(y) \mathrm{d}y = U, \; k_1 + k_2 = \frac{H_y^*(0)}{H_\delta} = u_0 \quad (2.1)$$

$$u_0 = 0.831957 + 1.54394 \cdot 10^{-2} \left(\frac{\delta}{a}\right) - 0.175235 \left(\frac{\delta}{a}\right)^2 + 7.66579 \cdot 10^{-2} \left(\frac{\delta}{a}\right)^3 - \quad (2.5)$$

$$-1.60908 \cdot 10^{-2} \left(\frac{\delta}{a}\right)^4 + 1.83817 \cdot 10^{-3} \left(\frac{\delta}{a}\right)^5 - 1.09529 \cdot 10^{-4} \left(\frac{\delta}{a}\right)^6 + 2.66537 \cdot 10^{-6} \left(\frac{\delta}{a}\right)^7$$

2.3 Utilization of PABCM to the inductance of plunger-type electromagnet computation

In the paper [36] is derived a formula to calculate the internal inductance of a plunger-type magnet, using the power approximation of boundary conditions method in two-dimensional space. The proposed formula is difficult to apply because of function:

$$F(\alpha, z) = \int_0^1 \frac{\cos[z(1-t)]}{t^{\alpha}} \mathrm{d}t; \qquad \alpha \in (0\,;1) \tag{2.8}$$

containing an improper integral. In this chapter is proposed a method ([40], [140]) for evaluating the function using MATHCAD software [178] and a numerical verification by finite element method (QUICKFIELD [179], [177] and FEMM [175]) of the inductance formula from the papers [36].

2.3.2 Computation of internal inductance of plunger-type electromagnet 1

The geometry of plunger-type electromagnet 1, for witch the inductance is computed, is presented in figure 2.5. The internal inductance per unit length (thickness) analytically computed $L'_{\text{int\_AN}}$, corresponding to the magnetic flux in electromagnet window (fig. 2.5) according to [36], can be written as:

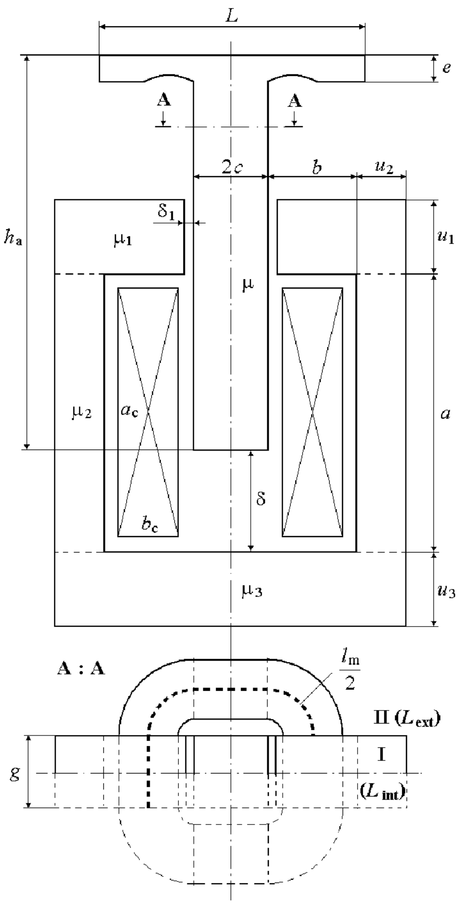

Fig. 2.5 - *Geometry of plunger-type electromagnet* 1

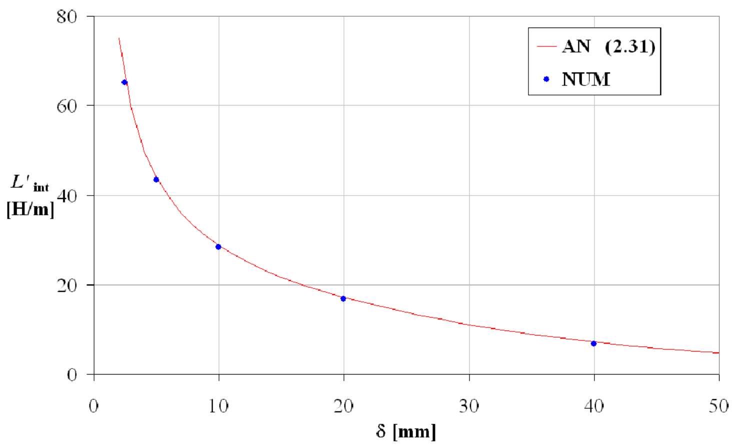

Fig. 2.6 - *Internal inductance per length unit, analytically computed by relationship* (2.31) (*line*) *and numerically by* QUICKFIELD, FEMM (*points*)

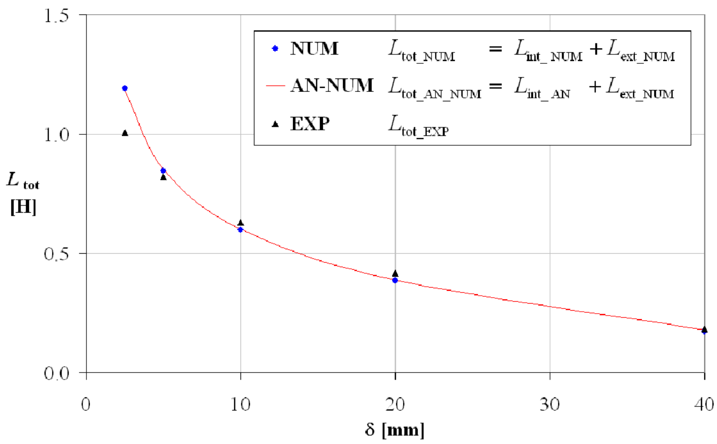

Fig. 2.7 - *Numerical results* (*points*), *analytic-numerically* (*line*) *and experimentally* (*triangles*) *for total inductance*

$$L'_{\text{int\_AN}} = 4\mu_0 w^2 \left[G + \frac{c}{\delta_e} + \frac{a_1 a + b_1 b}{2\delta_e} - \frac{a_2 a^2 + b_2 b^2}{6ab} \right] \tag{2.31}$$

In formula (2.31) the cross section of the coil is considered having the window size: $a_c \approx a$, $b_c \approx b$.

2.3.3 Numerical solution and experimental verification

In order to numerically verify the analytical expression of the internal inductance $L'_{\text{int\_AN}}$ (2.31) of plunger-type electromagnet 1 (Fig. 2.5), deduced by PABCM, was used 2-D FEM implemented in QUICKFIELD [179], [177] and FEMM [175] programs.

The internal inductance has been evaluated using the magnetic field energy corresponding to the interior domain (domain I, Fig. 2.5). The 2-D FEM analysis in MVP formulation was performed in magneto static regimes (1.42-1.45). In order to estimate the total inductance of the plunger-type electromagnet 1, the 2-D FEM analysis was extended to the outer magnetic core domain (domain II, fig. 2.5) corresponding to frontal parts of the coil.

$$L'_{\text{int\_NUM}} = 2\frac{2W'_{\text{m\_int}}}{I^2}, \qquad L'_{\text{ext\_NUM}} = 2\frac{2W'_{\text{m\_ext}}}{I^2}, \qquad I = J\,\frac{a_c b_c}{w} \tag{2.46}$$

Using internal and external values of inductances per unit length, analytically or numerically computed, the total inductance of the plunger-type electromagnet 1 is determined considering for internal inductance, the thickness g of the core and for external inductance, the difference between half-length of average turn ($l_m/2$) and thickness g (Fig. 2.5).

$$L_{\text{tot}} = L_{\text{int}} + L_{\text{ext}} = g\,L'_{\text{int}} + \left(\frac{l_m}{2} - g \right) L'_{\text{ext}} \tag{2.48}$$

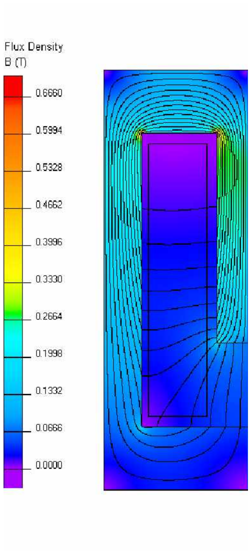

Fig. 2.8 - *Distribution of magnetic field density in interior domain for* δ = 20 *mm* (QUICKFIELD, 103,954 *nodes*)

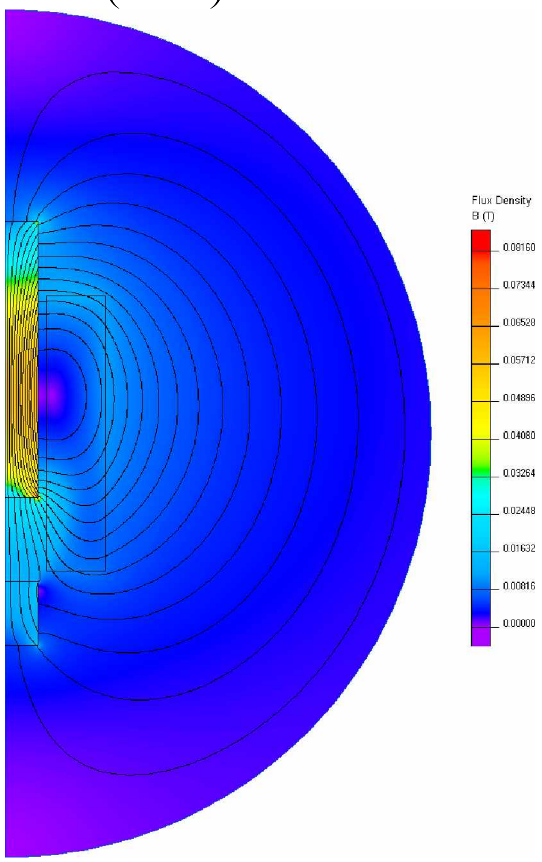

Fig. 2.9 - *Distribution of magnetic field density in exterior domain* δ = 20 *mm* (QUICKFIELD, 56,217 *nodes*)

Chapter III

STATIC CHARACTERISTIC OF A PLUNGER-TYPE ELECTROMAGNET

3.2 Numerical computation of electromagnetic forces

3.2.1 Maxwell stress tensor method (MTM)

The electromagnetic field theory [119] establishes that the force F acting on a body placed in the magnetic field, results by integration on body volume, of magnetic force density f, assumed known. An equivalent problem is considering a system of surface forces $\boldsymbol{T}_n$, called *magnetic* (*Maxwell*) *stress*, which, acting on a closed surface S around the body, produces the same resulting (Fig. 3.1):

$$F = \int_{V_S} f\,\mathrm{d}v = \oint_S \boldsymbol{T}_n \mathrm{d}s = \int_{V_S} \mathrm{div}[\mathrm{T}]\mathrm{d}v\,, \qquad \boldsymbol{T}_n = (\boldsymbol{Bn})\boldsymbol{H} - \frac{1}{2}(\boldsymbol{BH})\boldsymbol{n} \tag{3.1}$$

$\boldsymbol{T}_n$ is a vector quantity associated to external normal to surface S, with outward unit $\boldsymbol{n}$, by a tensor [T], with symmetric second-order components matrix, called *Maxwell's tensor* (*Maxwell stress tensor*).

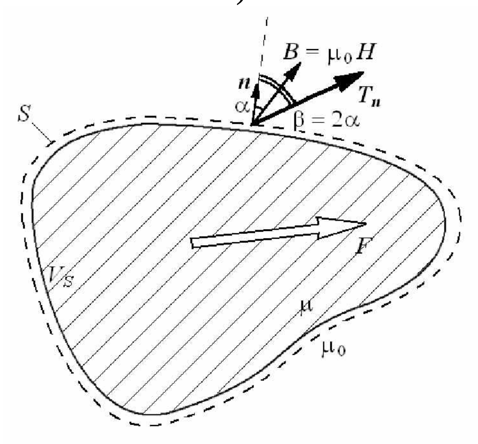

Fig. 3.1 - *Magnetic stress* $\boldsymbol{T}_n$

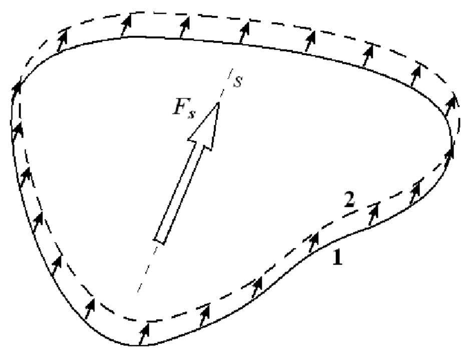

Fig. 3.2 - *Magnetic force* $\boldsymbol{F}_s$ *in s direction of virtual displacement*

3.2.2 Virtual work method (VWM)

Virtual work method (VWM) derived from the theorems of generalized forces in magnetic field, based on energy balance of an electromagnetic system. The electromagnetic field theory [119] establishes the expressions of generalized force F_s (force itself or torque) depending on the variation of magnetic energy (W_m) or complementary magnetic energy (co-energy) (W_m^*) of system with respect to generalized coordinate s (linear or angular displacement) in certain imposed mathematical conditions:

- constant magnetic flux Φ in derivative process: $$F_s = -\left.\frac{\partial W_m}{\partial s}\right|_{\Phi=\mathrm{ct.}} \tag{3.6}$$
- constant current i in derivative process: $$F_s = \left.\frac{\partial W_m^*}{\partial s}\right|_{i=\mathrm{ct.}} \tag{3.7}$$

3.3 Numerical determination of static characteristic of plunger-type electromagnet 2 and experimental verification

To numerically determine the static magnetic field, the finite element method (FEM) implemented in 3-D ANSYS program was used, in magnetic scalar potential formulation (MSP) and magnetic vector potential with edge elements (MVP-EE). In the case of MSP formulation, the electromagnetic force was computed by Maxwell's stress tensor method (MTM) and by virtual work method (VWM) and in the case of MVP-EE, by VWM [61].

For automation of numerical computation, the classic work with menus was dropped, adopting the alternative of creation of command files using the parameter language APDL (ANSYS Parameter Design Language) used by program ANSYS.

The electromagnetic force was measured using a tens sensor [61], [64] (Fig. 3.7) and simple procedures [51] (Fig. 3.8) for magneto-motive force in the range θ = 345.0-575.0 A.

This study points out the superiority of virtual work technique versus Maxwell stress tensor integration for electromagnetic force calculation from field solution obtained by finite element method.

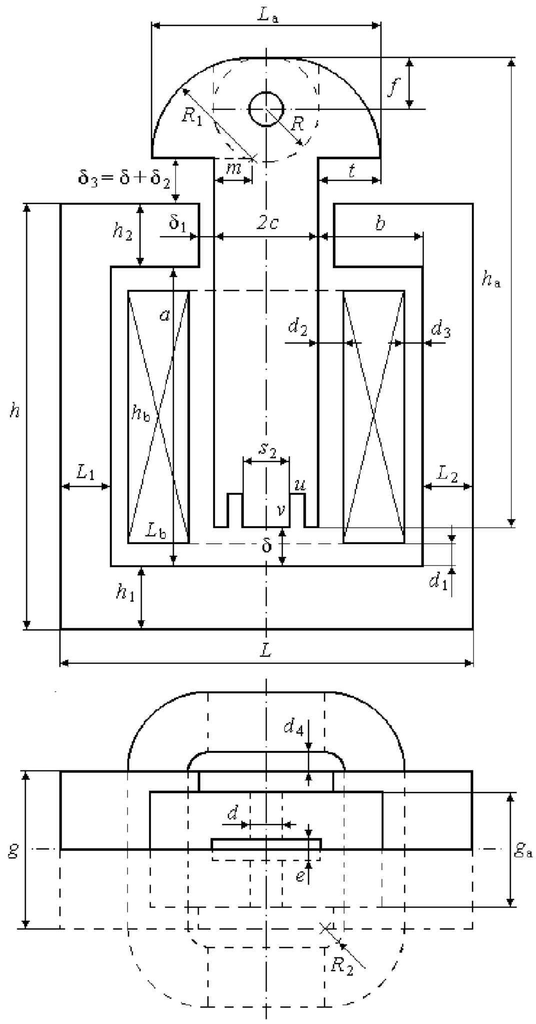

Fig. 3.6 - *Geometry of the plunger-type electromagnet* 2

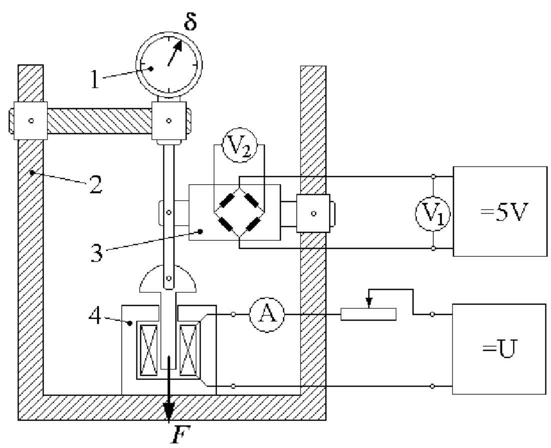

Fig. 3.7 - *Measurement scheme for magnetic force using a tens sensor*

1 - micrometer;
2 - support;
3 - tens sensor;
4 - electromagnet;
5 - additional weight.

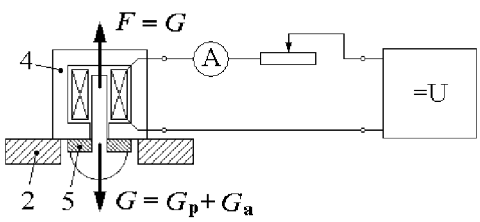

Fig. 3.8 - *Measurement scheme for magnetic force, balanced by the gravity force*

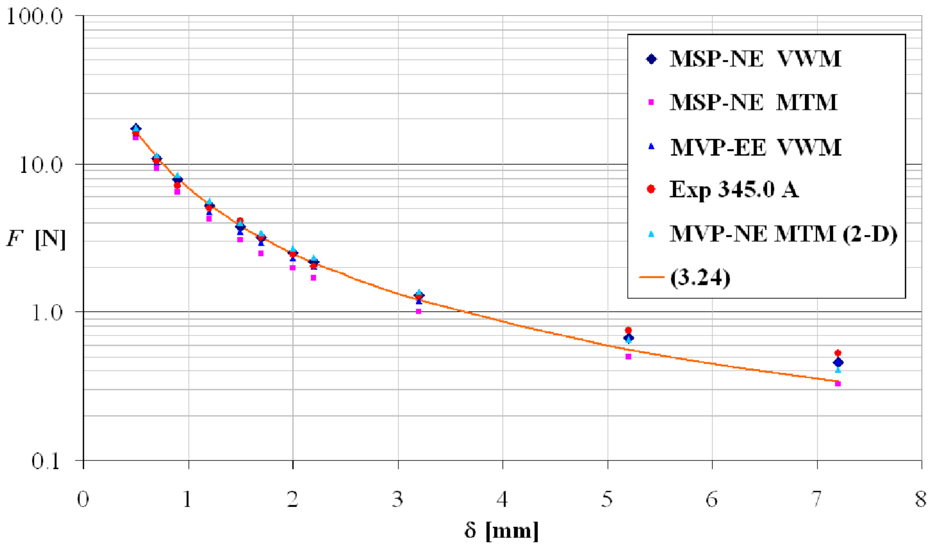

Fig. 3.11 - *Numerical and experimental static characteristics force - air-gap for* θ = 345.0 A

3.4 Theoretical determination of static characteristic of plunger-type electromagnet 2

Additional to numerical investigations on the evaluation of mechanical stress, analytical studies have been developed, providing sufficiently accurate solutions. Thus, the paper [51] recovered earlier theoretical research on the permeances computation using conformal mapping method [38], [37], [47], [50], providing 2-D simple and accurate analytical formulas for magnetic field computation and for force in various forms of electromagnetic devices. These formulas were applied to plunger- type electromagnet 2 (Fig. 3.6), in 2-D system [51].

The ratio k between λ_1 permeance corresponding main air-gap δ and λ_2 permeance of higher air-gap $\delta_3 = \delta + \delta_2$, can be expressed [51]:

$$k = \frac{\lambda_1(\delta)}{\lambda_2(\delta)} \approx \frac{\frac{c}{\delta} + 0.88}{\frac{c}{\delta} + \frac{h_2}{\delta_1} + \frac{t}{\delta_3} + 1.76} \tag{3.17}$$

The equivalent permeance was computed considering a series reluctances connection:

$$\lambda = \frac{\lambda_1 \lambda_2}{\lambda_1 + \lambda_2} \tag{3.22}$$

The electromagnetic force of plunger-type electromagnet 2 was derived:

$$F(\delta) = \mu_0 \frac{\theta^2}{\left(1 + \lambda(\delta)\frac{L_{\mathrm{Fe}}}{\mu_r c}\right)} g\lambda'(\delta) \tag{3.24}$$

The results are shown in Figure 3.11, compared with 3-D numerical solutions, which joined a 2-D solution by a FEM in MVP-EE formulation with MTM, observing the best matches on the whole range of analyzed air-gaps in comparison with the other methods.

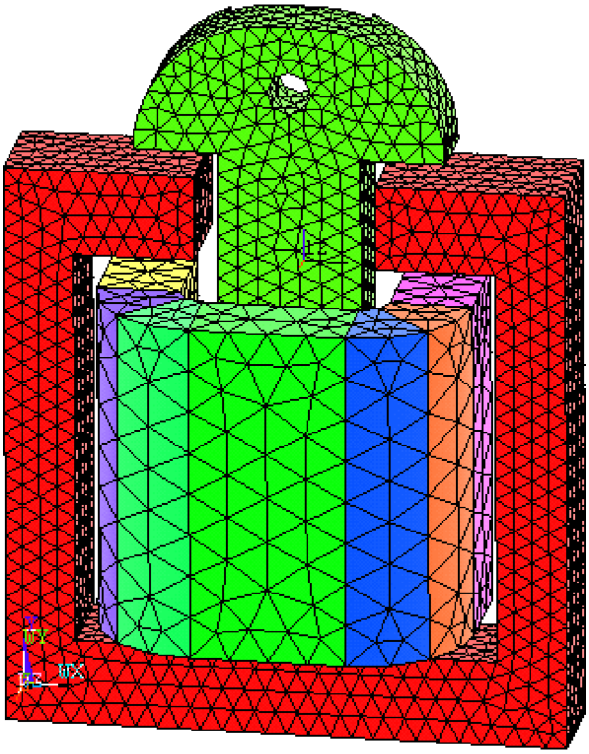

Fig. 3.15 - *Front perspective of the model with associated mesh* - MVP-EE *formulation* [61]

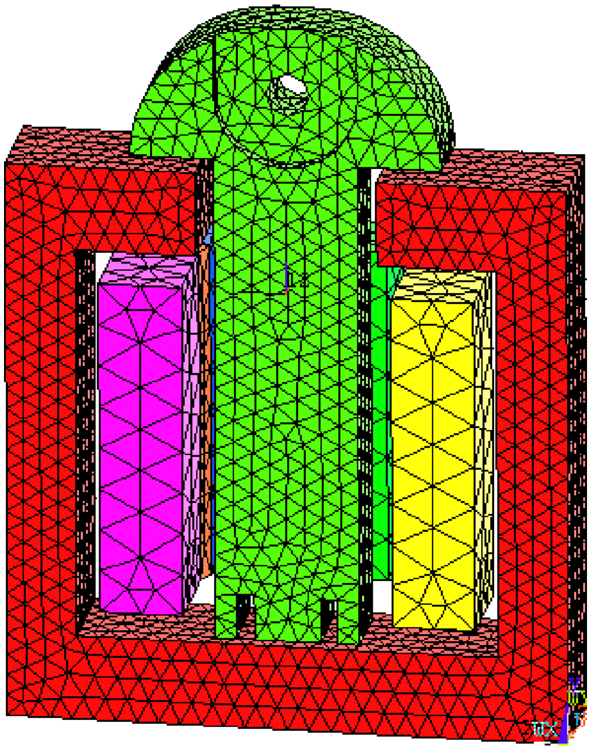

Fig. 3.16 - *Symmetry plane perspective of the model with associated mesh* - MVP-EE *formulation* [61]

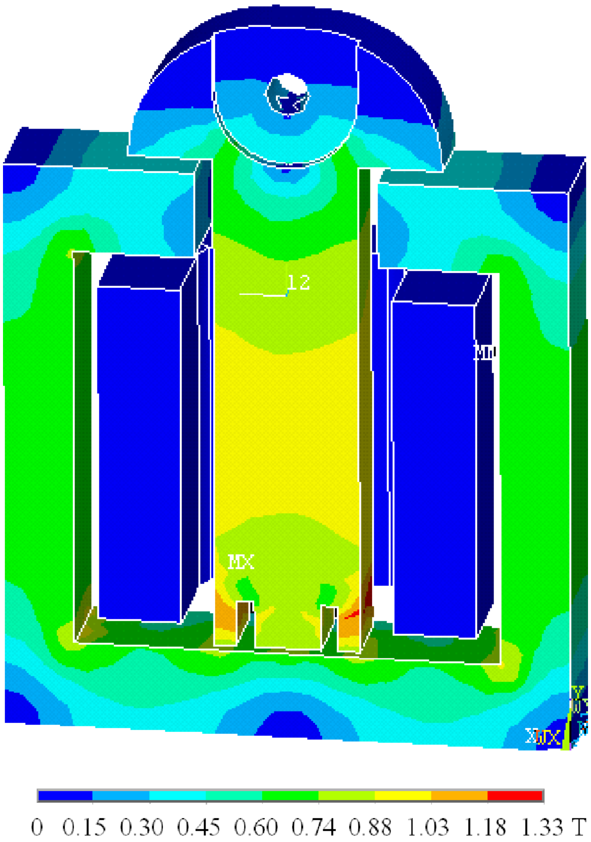

Fig. 3.17 - *Magnetic flux density on the symmetry plane and lateral faces*
(0.5 mm, 575.0 A, MVP-EE *formulation*) [61]

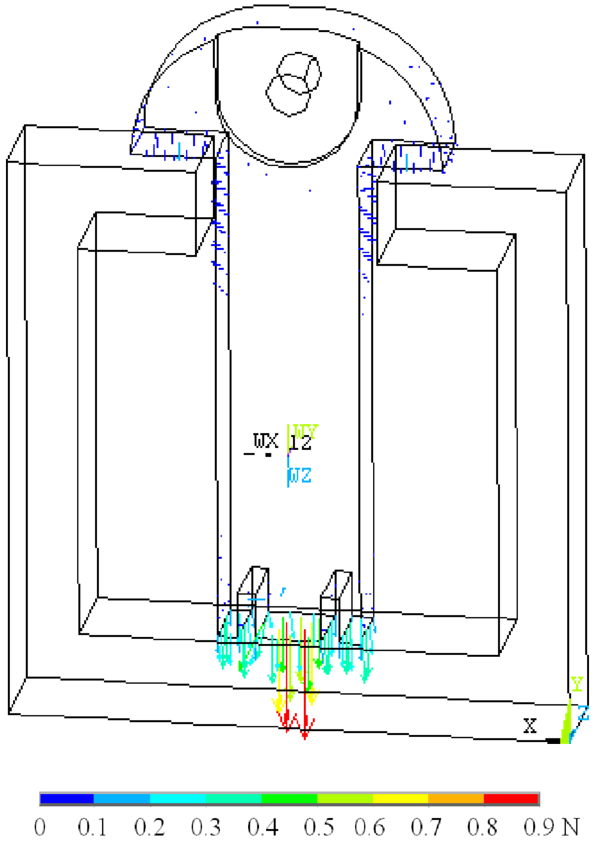

Fig. 3.18 - *Static electromagnetic force distribution*
(0.5 mm, 575.0 A, MVP-EE *formulation*) [61]

Chapter IV

LEAKAGE MAGNETIC FIELD AND MODELING LIGHTNING SURGES IN POWER MULTI-WINDING AUTOTRANSFORMER

4.3 Impedance voltage of the power multi-winding autotransformer

The power multi-winding three-phase autotransformer under investigation has rated powers of 400/400/80 MVA for voltage levels of 400/231/22 kV.

Let w_1, w_2, w_3 be the numbers of turns of the three principal windings of power autotransformer: primary, secondary and tertiary winding. The secondary winding is connected to the median (principal) tapping of the regulating winding, so that the phase secondary voltage for principal and marginal tappings is:

$$U_{2\mathrm{ph}} = U_{2\mathrm{phr}} \cdot \frac{w_2 + \alpha \frac{w_R}{2}}{w_2}, \qquad U_{2\mathrm{phr}} = \frac{U_{1\mathrm{r}}}{\sqrt{3}} \frac{w_2}{w_1 + w_2} \tag{4.22}$$

where $U_{1\mathrm{r}}$ is the primary rating line voltage and α is a coefficient depending on the tapping position of regulating winding, $-1 \leq \alpha \leq 1$, being zero for principal tapping.

4.3.1 Primary-secondary windings pair

To determine the short-circuit parameters of each pair of windings, the magnetic energy evaluation method was adopted. For primary-secondary windings pair, the magnetic field energy can be calculated for any arbitrary value of the primary line current $I_{1\mathrm{e}}$ (usually close to the primary rated current $I_{1\mathrm{r}}$).

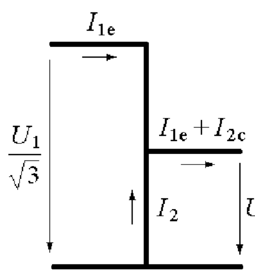

Fig. 4.4 - *Simplified autotransformer scheme*

For star connection, the phase current will be the same (fig. 4.4) and the corresponding secondary tapping currents ($I_{2\mathrm{c}}$) result from the equality of the primary and secondary magneto motive forces:

$$I_{2\mathrm{c}} = I_{1\mathrm{eph}} \cdot \frac{w_1}{w_2 + \alpha \frac{w_R}{2}}, \qquad I_{1\mathrm{eph}} = I_{1\mathrm{e}} \approx I_{1\mathrm{N}} \tag{4.23}$$

If W_{12} denotes the magnetic field mean energy per phase, produced by the currents $I_{1\mathrm{e}}$ and $I_{2\mathrm{c}}$, the referred to primary winding short-circuit reactance $X_{\mathrm{k}12}$ can be expressed in absolute values or in percentage of equivalent primary impedance $Z_{1\mathrm{N}}$, as:

$$X_{\mathrm{k}12} = \omega \cdot \frac{2W_{12}}{I_{1\mathrm{e}}^2}\ [\Omega], \qquad X_{\mathrm{k}12\%} = 100 \cdot \frac{X_{\mathrm{k}12}}{Z_{1\mathrm{N}}}\ [\%], \qquad Z_{1\mathrm{N}} = \frac{U_{1\mathrm{N}}}{\sqrt{3}\, I_{1\mathrm{N}}} \tag{4.25}$$

4.4 Numerical evaluation of the magnetic field energy and of the short-circuit reactance with FEMM program

4.4.1 2-D model and the boundary conditions

In the autotransformer window (Fig. 4.5), three ferromagnetic borders with zero tangential component of the magnetic field were considered. For the frontal part of the coils, the vertical border can be considered as zero potential magnetic line (A = 0). To study the approximation (A = 0) for symmetry axis (a - b), a harmonic analysis at commercial frequency was performed.

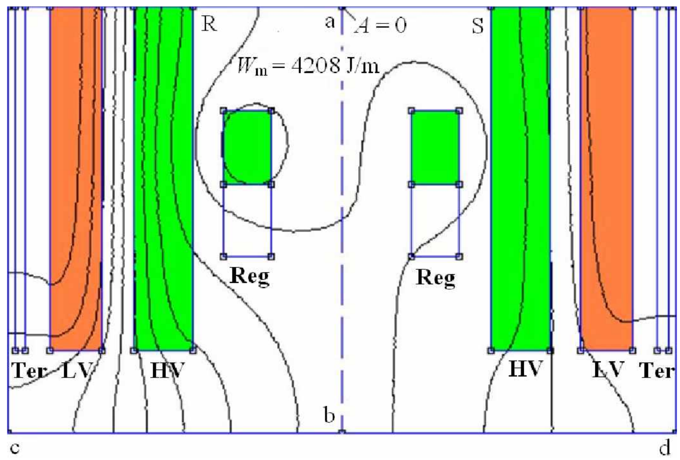

Fig. 4.5 - *Magnetic field pattern in autotransformer window with two phases, at* ***minus*** *tapping for* $\boldsymbol{i_R}$ **= max**

Phase	R	S
J_1 [A/mm^2]	0.799	- 0.400 - j0.692
J_2 [A/mm^2]	- 1.198	0.599 + j1.038
J_R [A/mm^2]	1,392	- 0,696 - j1.206

Tab. 4.1 - *Current densities corresponding to* R *and* S *phases, at* ***minus*** *tapping for* $\boldsymbol{i_R}$ **= max**

The analysis shows that the approximation (A = 0) can be enough well applied to the symmetry axis (a - b) of the autotransformer window (Fig. 4.5). If the current in T phase reaches its peak, the currents in R and S phases have equal values and the field distribution is completely symmetrical.

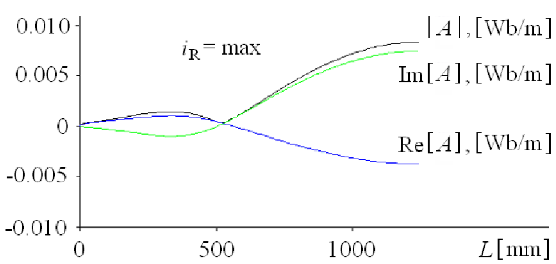

Fig. 4.6 - *Distribution of* MVP *along the symmetry axis* (a - b) *of autotransformer window, at* ***minus*** *tapping for* $\boldsymbol{i_R}$ **= max**

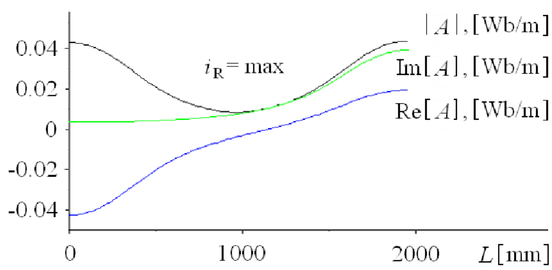

Fig. 4.7 - *Distribution of* MVP *along the bottom border* (c - d) *of autotransformer window, at* ***minus*** *tapping for* $\boldsymbol{i_R}$ **= max**

As it can be seen in Figures 4.6 and 4.7, the lowest value of potential module is obtained along the axis (a - b). The introduction of this border has the advantage of the possibility to apply a cylindrical model and of two times reduction of the nodes number.

4.4.2 2-D numerical results of short-circuit tests

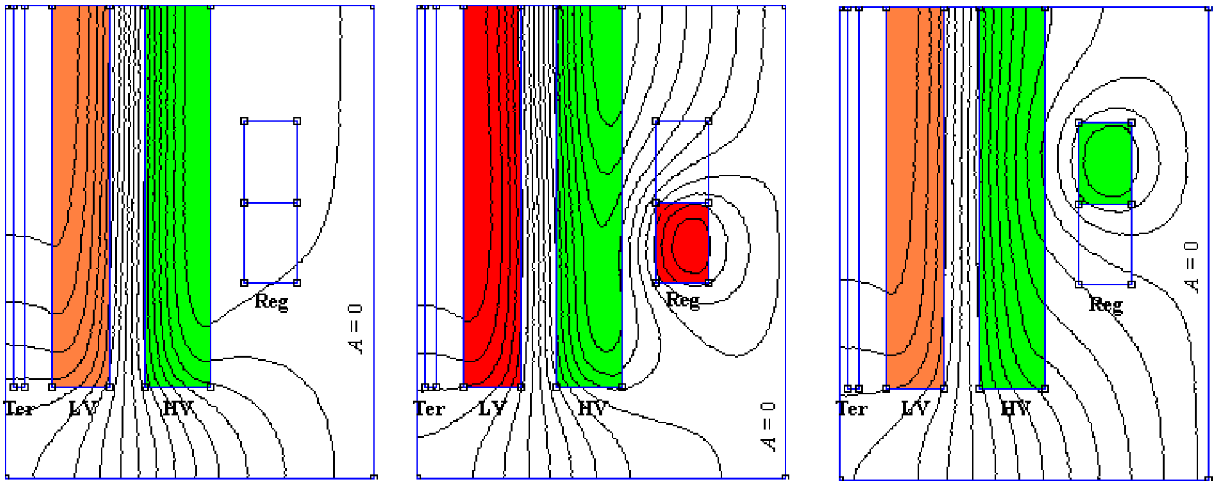

Principal tapping (0) **Plus tapping (+)** **Minus tapping (-)**

Fig. 4.11 - *Magnetic field pattern in inferior half autotransformer window for* ***primary-secondary*** *windings pair short-circuit test*

4.4 Numerical evaluation of the magnetic field energy and of the short-circuit reactance with ANSYS program

The analysis of the magnetic field in autotransformer has continued in the papers [65], [67] using 3-D FEM implemented in ANSYS program. Three formulations were used in the magneto static regime, MVP-EE [65], MVP-NE) [67] and MSP [67].

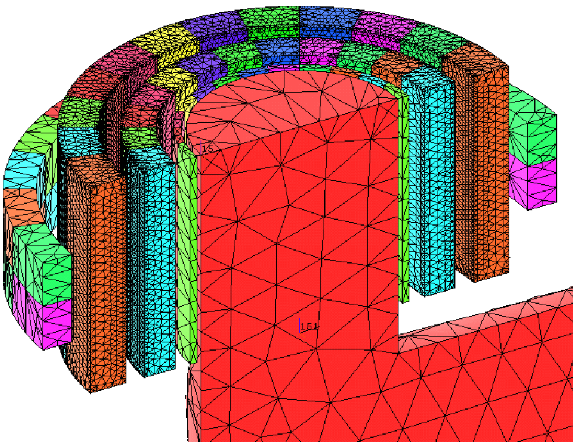

Fig. 4.14 - 3-D *model perspective with associated mesh*

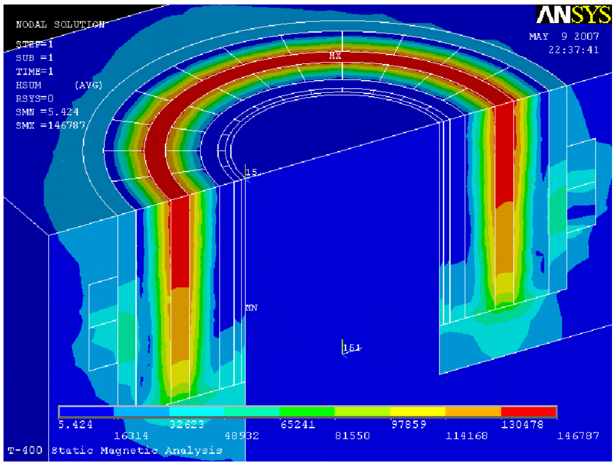

Fig. 4.15 - 3-D *magnetic field pattern in* MVP-EE *formulation, for* ***primary-secondary*** *windings pair short-circuit test, at* ***plus*** *tapping*

Pair	Tapp.	X_k [Ω]					X_k [%]			
		Exp	2D	3D			2D	3D		
			MVP-NE	MSP-NE	MVP-EE	MVP-NE	MVP-NE	MSP-NE	MVP-EE	MVP-NE
1-2	0	40.41	41.03	37.79	40.76	38.48	10.26	9.45	10.19	9.62
	+	29.56	28.87	27.64	29.11	27.35	7.22	6.91	7.28	6.84
	-	82.68	82.84	75.25	80.70	75.19	20.71	18.81	20.17	18.80

Tab. 4.7 - *Short-circuit reactance corresponding to short-circuit test for* ***primary-secondary*** *windings pair*

4.5.3 Optimization of 3-D simulations by memory management

The memory management has direct implications on solving time (t_s). When the complexity of the model requires, the operating system supplements the internal memory (physical, RAM) of PC with additional memory, allocated from virtual memory, located on the hard disk. This strongly affects the speed performance of the solving algorithm. So, just a minimum necessary amount of additional memory must be allocated [3].

Physical memory 1.5 GB Processor frequency 1.83 GHz	**No additional memory**			**Maximum PC capability**		
	MSP-NE	**MVP-EE**	**MVP-NE**	**MSP-NE**	**MVP-EE**	**MVP-NE**
Nodes	20,089	152,316	20,089	124,424	573,349	170,913
Elements	109,294	109,294	109,294	723,016	421,501	999,954
Equations	18,813	109,383	56,046	121,060	412,800	501,398
Additional memory	0 GB	0 GB	0 GB	1.5-2 GB	1.5-2 GB	2-3 GB
t_{s_real} **[sec]**	183	238	164	29,487	11,586	55,583
$t_{s\_estimate}$ **[sec] - for no RAM limit**				1,333	1,231	2,345
t_{s_real} **increasing rate**				22 x	10 x	24 x

Tab. 4.9 - *Solving time* (t_s) *for* "1-2 *plus*" *short-circuit test*

A limitation of solving time and a good precision were obtained by a different allocation of additional memory over the phases of pre-processing, processing, post-processing via a configuration file specific to ANSYS. The results presented in Table 4.9 show that utilization of additional memory in the range (1.5-3.0) GB, increases the solving time (10-24) times compared to the case of an unlimited internal memory.

4.6 Modeling lightning surges in the power multi-winding autotransformer

Both to the application of impulse voltages as well as of high frequency oscillating voltages, on the tapping of regulating winding and on the terminals, important over-voltages can appear, whose maximum values can exceed the maximum amount of applied voltages. The LC model study for the processes taking place in autotransformer windings during impulse voltage testing offers the opportunity to identify the constructive parameters influence on the level of the voltage impulse generated stress.

4.6.2 Self and mutual inductances for short-circuited tertiary winding

The self and mutual inductances were determined using the magnetic field in the autotransformer window for short-circuited and grounded tertiary winding. The field calculation was performed using the FEMM program [175]. The inductances are given by the expressions:

$$L_1 = \frac{\iiint_{S_1} A J_1 \,\mathrm{d}V}{I_1^2}, \qquad M_{12} = w_2' \frac{\iiint_{S_2} A \,\mathrm{d}V}{I_1} \tag{4.39}$$

where A represents magnetic vector potential, I_1 and j_1, the current and density current in the coil 1 (HV) with the cross-section S_1 and w'_2 and S_2, the turns density and the cross-section of the coil 2 (LV).

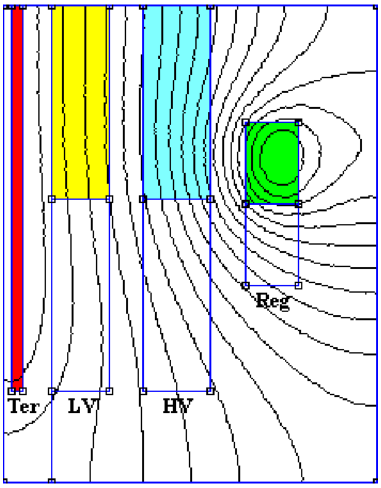

Fig. 4.18 - *Magnetic field pattern for current injected in upper half of regulating winding*

Current	**[A]**	290
Magneto motive force	**[kA]**	43.8
Current density	**[A/mm²]**	1.47; -1.37
$\iiint_{R/2} A\,J\,dV$	**[J]**	10208
$\iiint_{IT/2} A\,dV$	**[mWb·m²]**	9.34
$\iiint_{JT/2} A\,dV$	**[mWb·m²]**	2.53
$L_{Reg/2}$	**[mH]**	122
$M_{Reg/2\text{-}HV/2}$	**[mH]**	137
$M_{Reg/2\text{-}LV/2}$	**[mH]**	19

Tab. 4.12 - *Computed parameters and their values for current injected in upper half of regulating winding*

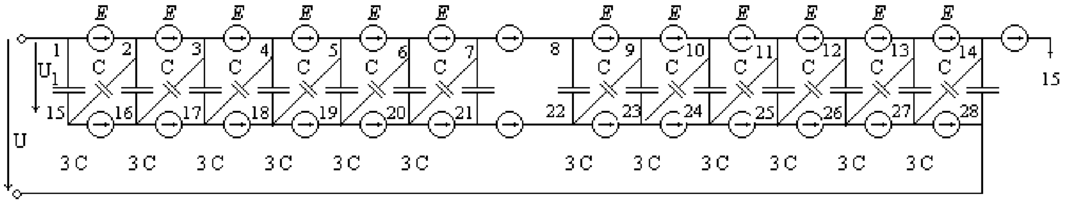

Fig.4.21 - *Wires capacitances for n = 14*

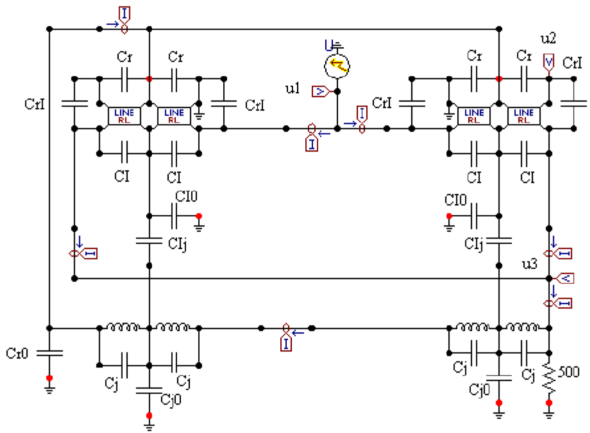

Fig. 4.22 - *Simplified scheme of autotransformer windings*

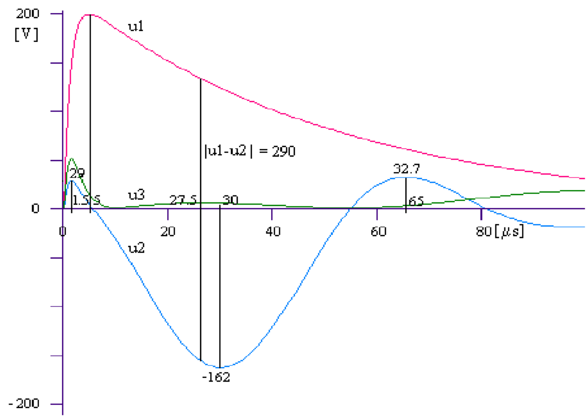

Fig. 4.23 - *Lightning surges in free end of regulating winding and in the common terminal* A_2 (u_2 *point and respectively* u_3 *point from simplified scheme*)

Chapter V

NUMERICAL SIMULATION OF TRANSIENT ELECTRIC AND MAGNETIC FIELDS IN RECTANGULAR SOLID BUS BARS

5.2 Analytical evaluation of magnetic field distribution

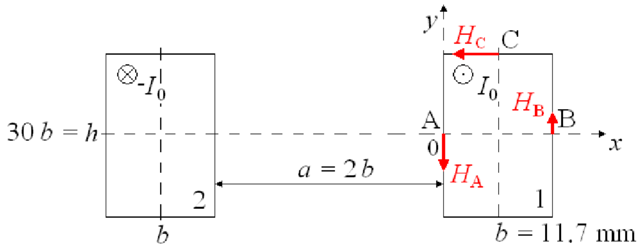

Fig. 5.2 - *System of two parallel current carrying bars*

5.2.2 Distribution of electric and magnetic fields at step current injection

In the case of current step injection $i(t) = I_0 \cdot 1(t)$ in a two bars system, short-circuited at the opposite end - equivalent to a sudden short-circuit apparition or to a direct current interruption - the magnetic and electric fields expressions in central part of bars ($y = 0$) are:

$$H_y(\xi,\theta) = H_{yA}\cdot\left[\xi(1+\eta) - 1 + \frac{2}{\pi}\sum_{k=1}^{\infty}(-1)^k \frac{\eta\sin(k\pi\xi) - \sin(k\pi(1-\xi))}{k} e^{-(k\pi)^2\theta}\right], \quad \theta = \frac{t}{\tau} \tag{5.15}$$

$$E_z(\xi,\theta) = \frac{E_0}{1+\eta}\cdot\left[1+\eta+2\sum_{k=1}^{\infty}(-1)^k\left[\eta\cos(k\pi\xi)+\cos(k\pi(1-\xi))\right]e^{-(k\pi)^2\theta}\right] \tag{5.16}$$

where
$$E_0 = \frac{I_0}{\sigma b h} \approx \frac{1+\eta}{\sigma b} H_{yA} \tag{5.17}$$

is the electric field in conductor in stationary regime [41].

If a step voltage $u(t) = U_0 \cdot 1(t)$ is applied, the magnetic and electric fields expressions in central part of bars (y = 0) can be written [41]:

$$H_y(\xi,\theta) = H_0\cdot\left[\xi - \frac{1}{1+\eta} - 2m\sum_{k=1}^{\infty}\frac{\eta\sin(\nu_k\xi) - \sin(\nu_k(1-\xi))}{\nu_k^2((m+1)\sin(\nu_k) + \nu_k\cos(\nu_k))}e^{-\nu_k^2\theta}\right] \tag{5.24}$$

$$E_z(\xi,\theta) = E_0\cdot\left[1 - 2m\sum_{k=1}^{\infty}\frac{\eta\cos(\nu_k\xi)+\cos(\nu_k(1-\xi))}{\nu_k((m+1)\sin(\nu_k)+\nu_k\cos(\nu_k))}e^{-\nu_k^2\theta}\right] \tag{5.25}$$

where ν_k are solutions of the equation [41]: $m(\eta + \cos\nu) = \nu\sin\nu$ (5.26)

5.3 Numerical simulation of transient electric and magnetic fields in the system of rectangular bus bars

For numerical simulation of the process of penetration of electric and magnetic fields in the system of parallel rectangular solid bars forming a circuit loop, was used 2-D finite element method implemented in FLUX [172] and FEMM [175] programs. The transient process itself and the stationary regime were investigated by FLUX 2D and the initial moment was analyzed using FEMM. The expulsion of the field lines from the conductor domain at analyzed moment was obtained by a trick involving the approximate cancellation of its relative permeability.

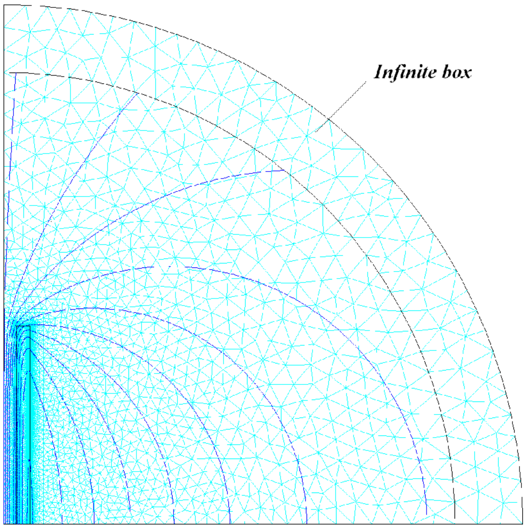

Fig. 5.3 - *Studied domain with associated mesh in* FLUX 2D (*stationary regime*)

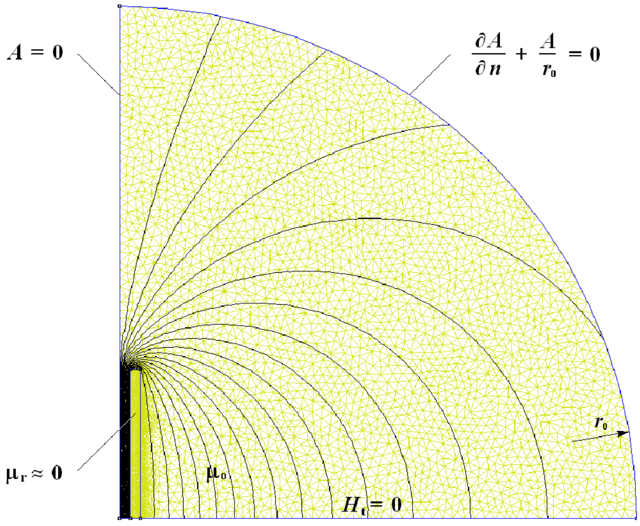

Fig. 5.5 - *Studied domain with associated mesh in* FEMM (*initial moment*)

5.3.4 Numerical evaluation of exterior magnetic field

FEMM investigation for very thin bars (b/a = 0.01) validates enough well the results of paper [48] in which the η ratio at initial moment (η_0) is computed by conformal mapping method (CMM), for configuration b/a = 0.

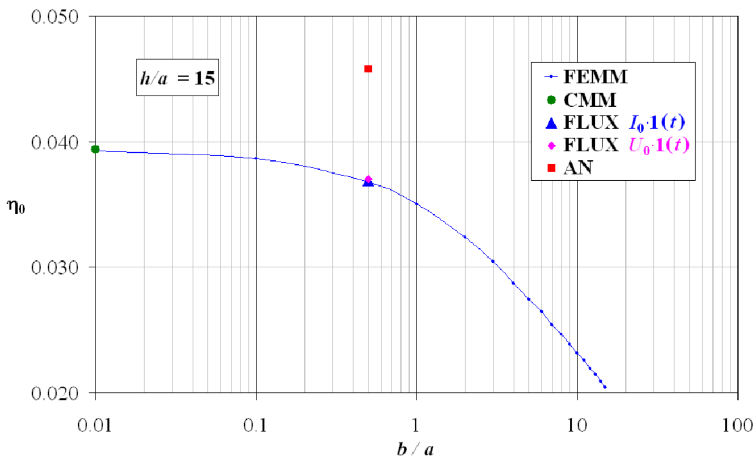

Fig. 5.6 - η_0 *ratio computed by different methods*

The transient magnetic field depends essentially on the initial field on the surface of conductors. In the paper [49] continue the analysis of this field started in [48] at current step injection in the bar system in Fig. 5.2. For the exact formulas obtained in [48] for infinitely small thickness bars, simple approximations are proposed, containing the factor used by Dwight to determine the electrodynamic forces between the bars (5.27), thus extending the applicability domain to small thickness bars:

$$\eta_0(x) = \left|\frac{H_{\mathrm{yB}}}{H_{\mathrm{yA}}}\right| = \frac{\dfrac{\pi}{2} - \mathrm{arctg}\left(\dfrac{x}{2}\right)}{\dfrac{\pi}{2} + \mathrm{arctg}\left(\dfrac{x}{2}\right)}, \qquad x = \frac{h+b}{a}, \qquad b < h \tag{5.27}$$

The problem is also solved by numerical conformal mapping, using Schwartz-Christoffel module (SC) of the MATLAB program.

Similarly to the ratio η of the tangential components of magnetic field on the lateral sides, is defined the ratio η_b of tangential components of the points C and A (Fig. 5.2) for whose average is proposed the formula:

$$\eta_{b\,\mathrm{med}}\left(\frac{b}{a}\right) = \left|\frac{H_{\mathrm{xC}}}{H_{\mathrm{yA}}}\right| = \frac{\pi - 4\,\mathrm{arctg}\left(\dfrac{b}{2a+b}\right)}{\pi + 4\,\mathrm{arctg}\left(\dfrac{h}{2a+3b}\right)} \cdot \left[1 + \frac{h}{100a} + \frac{b}{a}\left(0.03 + \frac{h}{2000a}\right)\right] \tag{5.29}$$

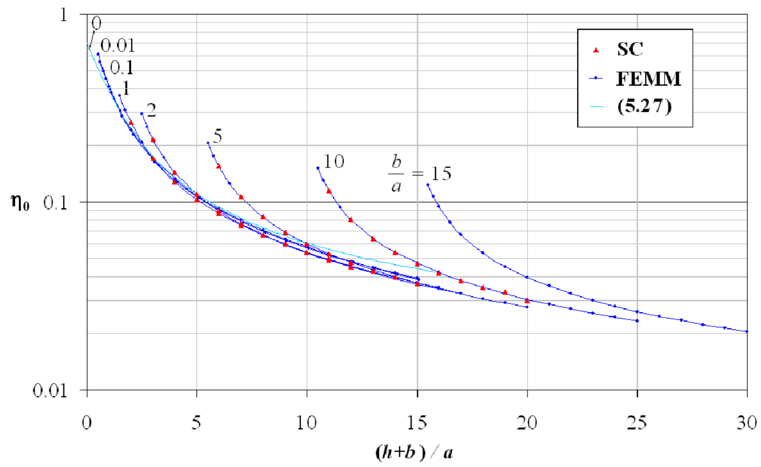

Fig. 5.11 - *Influence of bars system geometry* (*h/a, b/a*) *on* η_0 *ratio*
- *numerical* (SC, FEMM) *and analytical* (5.27) *results* -

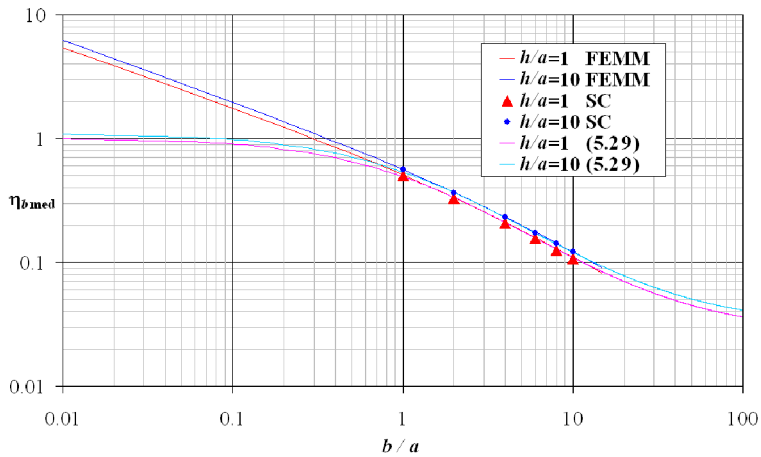

Fig. 5.14 - *Influence of bars system geometry* (*h/a, b/a*) *on* η_b *ratio*
- *numerical* (SC, FEMM) *and analytical* (5.29) *results* -

5.3.5 Numerical evaluation of electric and magnetic fields distribution at step current injection

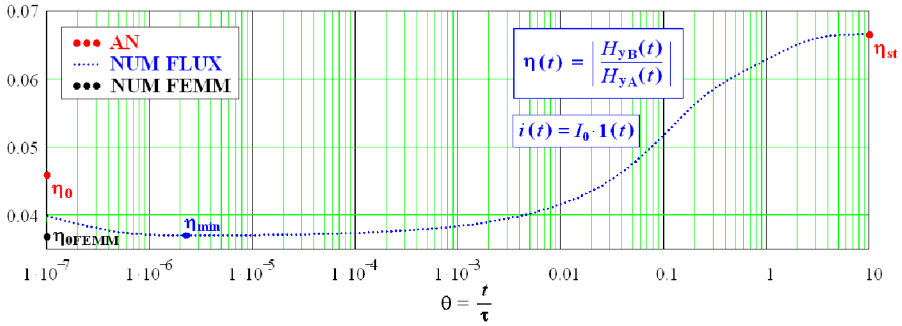

Fig. 5.15 - *Evolution of ratio* η *along the transient process at current step injection*

In the paper [41] the tangential component of the magnetic field and longitudinal electric field component were computed based on analytical equations (5.22), (5.23) using the same value of η_{st} ratio for all analyzed moments. In this paper is proposed a mixed analytic-numerical solution (Fig. 5.17 and 5.19), based on the same equations, but using a variable η ratio, resulting from FLUX 2D numerical simulation (Fig. 5.15).

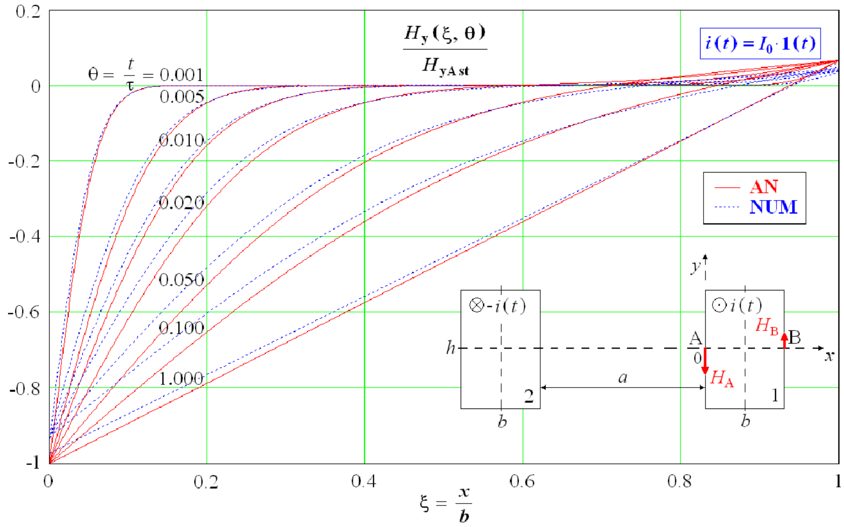

Fig. 5.16 - *Numerical and analytical results for transient magnetic field in conductor* 1 *at current step injection, for h/b* = 30 *and a/b* = 2

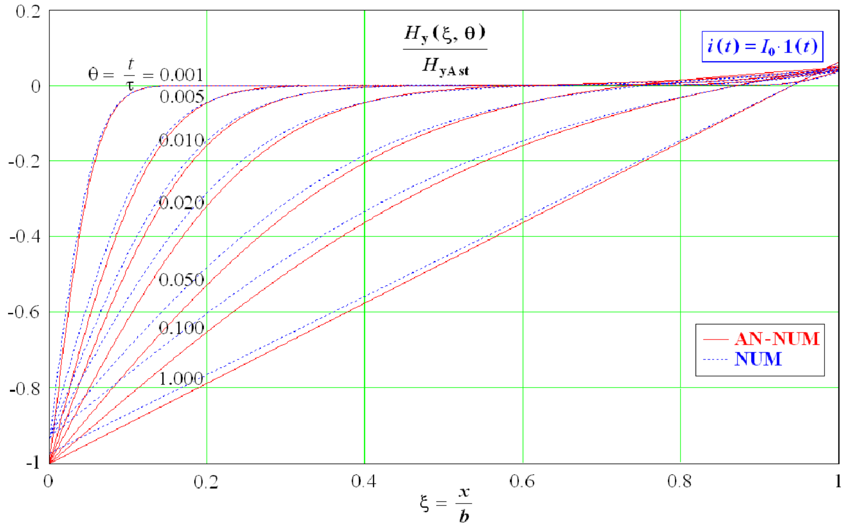

Fig. 5.17 - *Numerical and analytic-numerical results for transient magnetic field in conductor* 1 *at current step injection, for h/b* = 30 *and a/b* = 2

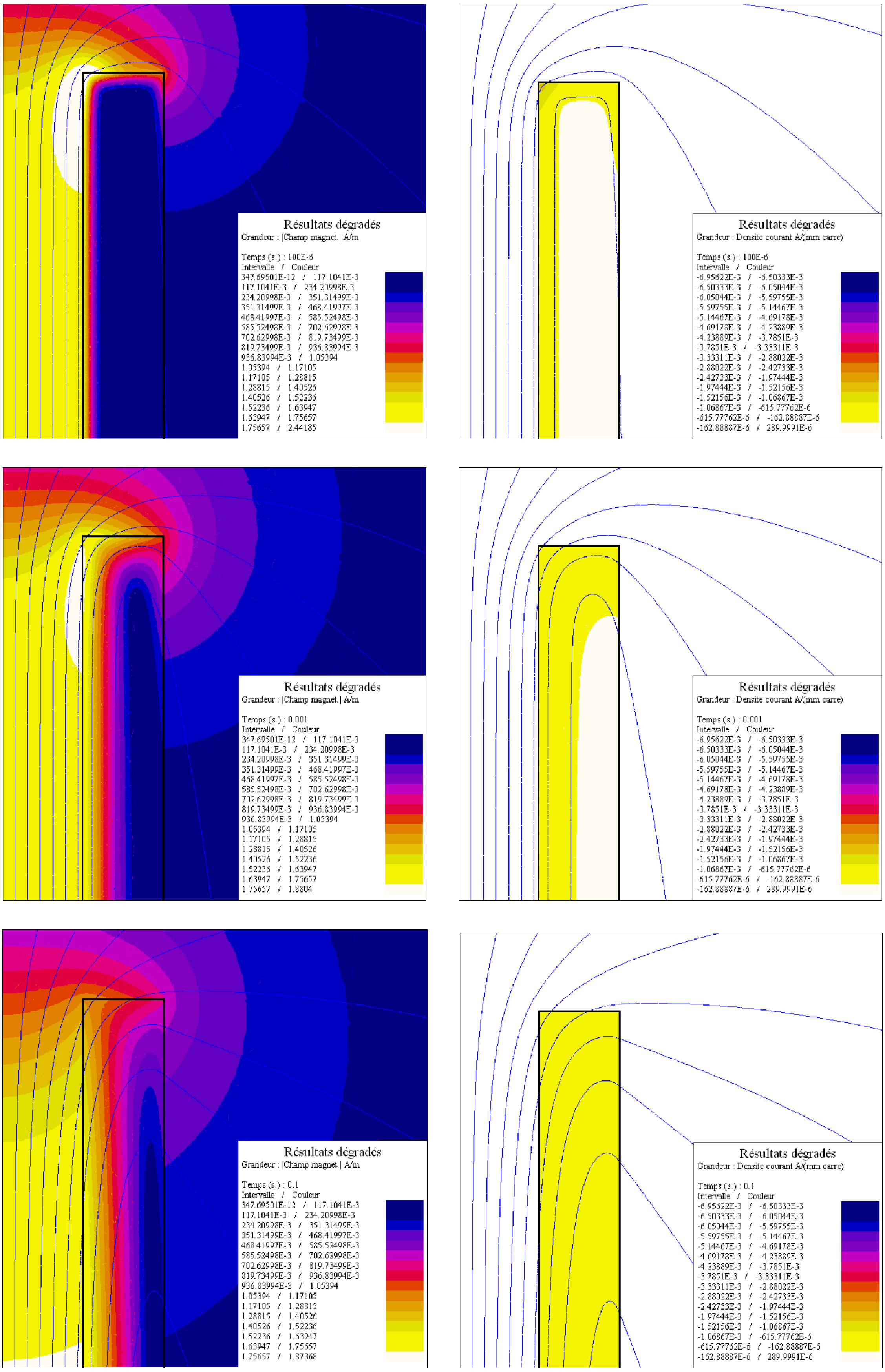

Fig. 5.29 - *Distribution of magnetic field* (*left*) *and of current density* (*right*) *for* $\theta = 10^{-2}$, $\theta = 10^{-1}$, $\theta = 10$, *at step current* (FLUX 2D)

Chapter VI

NUMERICAL DETERMINATION OF TRANSIENT PARAMETERS OF A SYSTEM OF RECTANGULAR SOLID BUS BARS

6.1 Transient parameters of the linear electrical circuits

6.1.4 Transient parameters of a non-filiforme and with additional losses circuit element

6.1.4.4 Integral relationships between instantaneous values of currents and voltages

The integral equations of current and voltage ($\varepsilon > 0$, arbitrary little) for the non-filiforme circuit elements and with additional losses are respectively:

$$u(t) = l(0_+)\frac{\mathrm{d}i}{\mathrm{d}t} + \frac{\mathrm{d}}{\mathrm{d}t}\int_0^t r(t-\xi)i(\xi)\mathrm{d}\xi + u_0(t) = r_0 i + l(0_+)\frac{\mathrm{d}i}{\mathrm{d}t} + \frac{\mathrm{d}}{\mathrm{d}t}\int_0^{t-\varepsilon}\frac{\mathrm{d}l(t-\xi)}{\mathrm{d}t}i(\xi)\mathrm{d}\xi + u_0(t) \quad (6.70)$$

$$i(t) = c(0_+)\frac{\mathrm{d}u}{\mathrm{d}t} + \frac{\mathrm{d}}{\mathrm{d}t}\int_0^t g(t-\xi)u(\xi)\mathrm{d}\xi + i_0(t) = g_0 u + c(0_+)\frac{\mathrm{d}u}{\mathrm{d}t} + \frac{\mathrm{d}}{\mathrm{d}t}\int_0^{t-\varepsilon}\frac{\mathrm{d}c(t-\xi)}{\mathrm{d}t}u(\xi)\mathrm{d}\xi + i_0(t) \quad (6.71)$$

6.1.4.5 Experimental determination of transient parameters

At *current step* injection $i(t) = 1(t)$, respectively, at *voltage step* application $u(t) = 1(t)$, the relationships (6.70), (6.71) become :

$$u(t) = l(0_+)\delta(t) + r(t) = r_0 \cdot 1(t) + \frac{\mathrm{d}l(t)}{\mathrm{d}t}, \qquad \int_{0-\varepsilon}^{t} u(t)\mathrm{d}t = r_0 t + l(t) \quad (6.80)$$

$$i(t) = c(0_+)\delta(t) + g(t) = g_0 \cdot 1(t) + \frac{\mathrm{d}c(t)}{\mathrm{d}t}, \qquad \int_{0-\varepsilon}^{t} i(t)\mathrm{d}t = g_0 t + c(t) \quad (6.81)$$

At *current ramp* injection $i(t) = t\cdot 1(t)$, respectively, at *voltage ramp* application $u(t) = t\cdot 1(t)$, the relationships (6.70), (6.71) become :

$$u(t) = l(0_+)\cdot 1(t) + \int_{0-\varepsilon}^{t} r(t)\mathrm{d}t = r_0 \cdot t + l(t), \qquad \frac{\mathrm{d}u(t)}{\mathrm{d}t} = l(0_+)\cdot\delta(t) + r(t) \quad (6.84)$$

$$i(t) = c(0_+)\cdot 1(t) + \int_{0-\varepsilon}^{t} g(t)\mathrm{d}t = g_0 \cdot t + c(t), \qquad \frac{\mathrm{d}i(t)}{\mathrm{d}t} = c(0_+)\cdot\delta(t) + g(t) \quad (6.85)$$

The determination of transient resistance and conductance can be convenient in experimental conditions of step signals application, when, for a capacitive element ($l(0_+) = 0$) or inductive element ($c(0_+) = 0$), these parameters are identified with the applied signals:

$$r(t) = u(t) - l(0_+)\delta(t)\Big|_{i(t)=1(t)} = u(t)\Big|_{i(t)=1(t),\ t>0} \quad (6.92)$$

$$g(t) = i(t) - l(0_+)\delta(t)\Big|_{u(t)=1(t)} = i(t)\Big|_{u(t)=1(t),\ t>0} \quad (6.93)$$

6.2 Utilization of FLUX program in determination of transient parameters of the system of rectangular solid bus bars

6.2.2 Determination of transient resistance and inductance at step current injection

At current step injection $i(t) = I_0 \cdot 1(t)$, for $t \geq 0$, the relationship (6.80) [140] links the transient resistance and the transient inductance:

$$u(t) = I_0\left[l(0_+)\delta(t) + r(t)\right] = I_0\left[r_0 \cdot 1(t) + \frac{\mathrm{d}l(t)}{\mathrm{d}t}\right], \qquad t \geq 0 \qquad (6.99)$$

Using directly the numerical value of voltage at step current $u_{\text{step\_crt\_NUM}}(t)$, from the first equality and for $t > 0$, results *the transient resistance at step current, from voltage* $r_{\text{step\_crt\_U}}(t)$.

$$r_{\text{step\_crt\_U}}(t) = \left.\frac{u_{\text{step\_crt\_NUM}}(t)}{I_0}\right|_{t>0} \qquad (6.100)$$

The second equality in (6.99) suggests another way to obtain transient resistance using *the numerical value of the transient inductance at step current* $l_{\text{step\_crt\_NUM}}(t)$ given by FLUX (total inductance). The result was suggestively called *transient resistance at step current from inductance* $r_{\text{step\_crt\_L}}(t)$.

$$r_{\text{step\_crt\_L}}(t) = r_0 + \frac{\mathrm{d}l_{\text{step\_crt\_NUM}}(t)}{\mathrm{d}t} \qquad (6.101)$$

Mutually, from the second equality can be approximately deduced the transient inductance from transient resistance, using the numerical value of inductance in stationary regime for its limit at infinity L_∞ and the value $r_{\text{step\_crt\_U}}(t)$ for transient resistance $r(t)$:

$$l(t) = L_\infty - \int_t^\infty \left(r(t) - r_0\right)\mathrm{d}t \approx L_{\text{st}} - \int_t^{10\cdot\tau} \left(r_{\text{step\_crt\_U}}(t) - r_0\right)\mathrm{d}t = l_{\text{step\_crt\_R}}(t) \qquad (6.103)$$

The result was generically called *transient inductivity at step current from resistance* $l_{\text{step\_crt\_R}}(t)$.

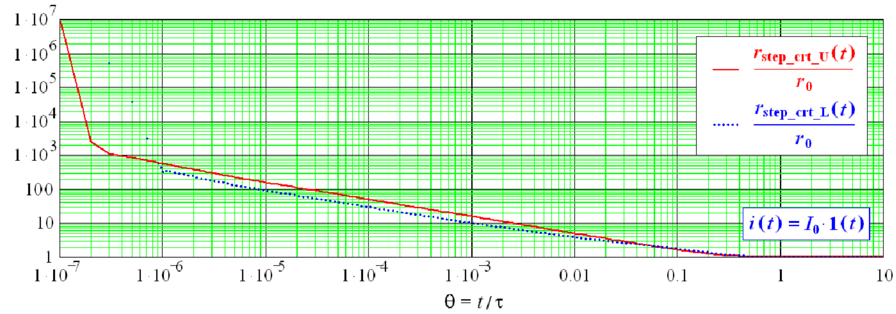

Fig. 6.8 - *Transient resistance at step current: solid line* (6.100), *dot line* (6.101)

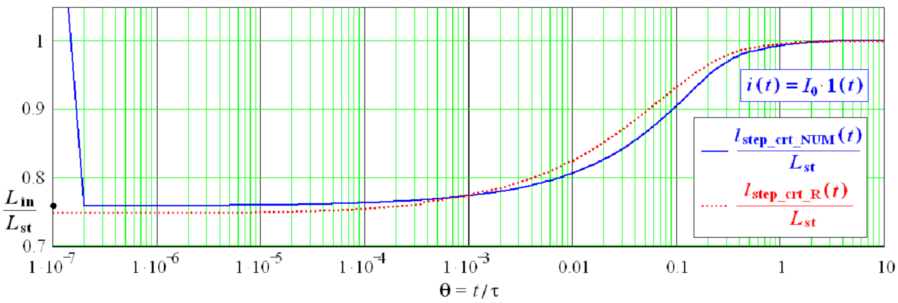

Fig. 6.9 - *Transient inductance at step current: solid line* (FLUX), *dot line* (6.103), *initial inductance: point* (6.109)

Chapter VII

ORIGINAL CONTRIBUTIONS AND CONCLUSIONS

Author's original contributions to modeling the fields and transient regimes in electrical equipments are structured on the chapters.

In **Chapter II** is proposed an experimental and numerical verification of *power approximation of boundary conditions method* (PABCM) developed in [32], [33], [35] in the evaluation of total inductance of a plunger-type electromagnet (Fig. 2.5). The author's contributions in this verification follow:

- Based on PABCM, in the paper [36], in the assumption of fitting coil dimensions with electromagnet window, was derived an analytical expression of the internal inductance per unit length L'_{int_AN} (2.31) (domain I, corresponding to the magnetic core with thickness g, Fig. 2.5) for 2-D case, which is difficult to apply because it contains an improper integral $F(\alpha, z)$ (2.21). The author proposes its computation using MATHCAD program [178];
- To evaluate the total inductance of the electromagnet L_{tot} were taken into account two components: internal inductance L_{int} (domain I, Fig. 2.5) obtained by multiplying the internal inductance per unit length L'_{int} by the thickness g of magnetic core and external inductance L_{ext} (domain II, outer magnetic core domain, corresponding to frontal parts of the coil, Fig. 2.5) obtained by multiplying the external inductance per unit length L'_{ext} by difference between half-length of average turn (l_m / 2) and the thickness g (Fig. 2.5).
- The two components were numerically evaluated based on magnetic energy stored in corresponding domains, determined by FEM in magneto static regime implemented in QUICKFIELD [179] [177] and FEMM [175] programs. The average relative error of numerical solution versus analytical solution for the internal inductance per unit length L'_{int} is 2.47%, validating the analytical formula (2.31) to calculate the internal inductance.
- The analytical and numerical evaluation of internal inductance and numerical evaluation of the external inductance by two programs for 2-D FEM analysis led to two solutions for the total inductance, one purely numerical witch presents very small average deviations versus experimental data (0.78%) and an other solution, analytical-numerical, with errors of 1.67%. The accuracy of the results containing the analytical formula (2.31) once again confirms its accuracy.
- It were justified some results errors being made useful recommendations. The large differences between experimental data and those calculated for small air-gaps can be explained by distorted form of the plunger, whose sides are not flat as in Figure 2.5. Another possible errors source can be the simplified geometry of "I" form of plunger versus "T" real form (Fig. 2.5). The analytical and numerical solutions accuracy can be improved by removing the simplified geometric assumptions and, concerning only numerical solution, by 3-D approach for exact geometric configuration description.

Chapter III presents the results of theoretical and experimental investigations on a plunger-type electromagnet to test the effectiveness of analytical and numerical methods for calculating the developed force.

Earlier theoretical research [38], [37], [47], [50] using *conformal mapping method* (CMM) provided simple and precise analytical formulas for 2-D permeances calculation, useful for obtaining of an analytical expression for the electromagnetic force (3.19). The author has created 3-D numerical models of a plunger-type electromagnet (Fig. 3.6) and experimental determinations were performed to validate the own results and the analytical ones. The contributions in these investigations are presented below:

- The numerical method used for analysis is the finite element method (FEM), which is most suitable for the techniques of determining the force. Two formulations of 3-D FEM in magneto static regime were adopted: *the magnetic scalar potential formulation with nodal elements* (MSP-NE) and *the magnetic vector potential formulation with edge elements* (MVP-EE). Two classical techniques to obtain the global force from the field solution were chosen: *the Maxwell stress tensor method* (MTM) and *the virtual work method* (VWM). The adopted formulations in conjunction with one or both techniques, implemented in the ANSYS program [171] led to obtain three numerical solutions for static characteristic of plunger-type electromagnet: MSP-NE MTM, MSP-NE VWM and MVP-EE VWM.
- To automate the calculation, the classic work with menus was dropped, adopting the alternative of creation of command files using the parameter language APDL of ANSYS program and to reduce the execution time of these files the *batch mode* was adopted minimizing the required hardware resources.
- The electromagnetic force was experimentally determined for a particular range of air-gap, using a tens sensor for smaller air-gaps and simple procedures of gravity plunger determination, applied to higher air-gaps, when the saturation effect is negligible.
- The obtaining of parallel results (Fig. 3.9) allowed the comparison of the methods based on measurements. Average relative error of analysis versus experimental data shows that the most accurate solution is given by MSP VWM, with 0.08%, followed by MVP-EE VWM formulation with 6.17%, the least precise formulation being obtained by MSP MTM, with 20.27% (Fig. 3.10). This study pointed out the superiority of virtual work technique compared to Maxwell stress tensor integration for electromagnetic force calculation from 3-D FEM field solution. *The magnetic vector potential formulation with nodal elements* (MVP-NE) was also used in conjunction with both techniques MTM and VWM, but the results have proved wrong. However, its 2-D implementation in FEMM program [175] in conjunction with MTM is in good agreement with experimental data (Fig. 3.9) (average relative error of 4.00%). Also, the average relative error of the force obtained with the analytical formula (3.24) compared to measurements is of 3.89%, witch is its validation (Fig. 3.9).
- Another criterion of comparison between methods was the solution convergence versus the number of used finite elements and the size of elements in air-gap that have great influence on force accuracy. The results show a faster convergence of VWM compared to MTM requiring a finer mesh.

In **Chapter IV** has been studied the leakage magnetic flux in a three phase power autotransformer 400/400/80 MVA, 400/231/22 kV, with primary, secondary, tertiary and regulating windings, with multiple tappings, resulting 2-D and 3-D numerical models.

The autotransformer behavior at the application of lightning surges was also analyzed, aiming the over voltages level on the tappings of regulating winding. The considerable size of 3-D numerical simulations led to investigations for their optimization, concerning the solving time reduction and accuracy increasing, up to hardware resources. The author's contributions in these studies are pointed out below:

- Since the impedance voltage for secondary tapping of regulating winding can not be evaluated using simple formulas, derived under the assumption of straight lines of magnetic flux, the author has considered the real pattern of magnetic field obtained by FEM. Thus, two numerical models were obtained, a 2-D model using FEMM program [175] and a 3-D one using ANSYS program [171], assuming a static magnetic regime which approximates enough well the regime of commercial frequency, taking into account the small sections of the conductors.

- To obtain the 2-D model, a preliminary study for necessary boundary conditions was performed. For the frontal part of the coils, on the vertical border, a small skin depth should be considered, due to aluminum or copper screen of the autotransformer tank. However, at commercial frequency, the magnetic field determined in these conditions is practically identical to the static field corresponding to zero frequency and the vertical frontal border can be considered as a zero magnetic potential line ($A = 0$).
- For the other borders, a FEMM analysis was performed in harmonic regime at commercial frequency, at two moments delayed by a quarter of period, aiming the magnetic vector potential (MVP) values along the symmetry line of the autotransformer window, compared to its values on the bottom border of the window (Fig. 4.5, 4.10). The results had showed extremely low values (Fig. 4.6-4.9), suggesting consideration of symmetry lines of the windows as zero potential magnetic flux lines.
- The last approximation is also sustained by the equality of magnetic field energies per unit length, calculated at the two moments.
- Another confirmation is given by the recalculation of the energy, applying the approximation to the symmetry axis, which proved to be only 0.50% lower.
- Considering the symmetry lines of the autotransformer windows as zero magnetic potential flux lines, like the flux lines from the frontal parts of windings, in the vicinity of the screened tank, has allowed the use of a cylindrical model, very economical in terms of numerical computation. The FEMM axi-symmetric solution in magneto static regime for the short-circuit reactance corresponding to principal and marginal tappings of regulating winding, agree with the experimental data with errors less than 3.00% (Table 4.8).
- The field problem was solved in 3-D using three formulations of FEM: MVP-EE, MVP-NE and MSP-NE, implemented in ANSYS for magneto static regime that led to results that deviate on average 1.00%, 5.83% and 8.34% from experimental values. Despite of simplifying assumptions, the 2-D axisymmetric solution in MVP-NE formulation, with an average relative error of 0.11%, ranks first in terms of accuracy (Table 4.8).
- Again, to automate the calculation, the work with commands files was adopted, using the parameter language APDL.
- Using ATP-EMTP software package [173], [174] and FEMM, the power multi-winding autotransformer behavior was studied at lightning surges application, considering a L-C simplified model of the windings, with short-circuited tertiary winding, aiming the level of over voltages that appear on the free end of regulating winding.
- The self and mutual inductances were determined with FEMM program in axisymmetric approach for short-circuited and grounded tertiary winding. Have been neglected the mutual inductances between the regulating and low voltage windings, because of its relatively low value, facilitated by the screen effect of the high voltage winding, located between them. Have been also neglected the mutual inductance between the high and low voltage windings. The distributed nature of the windings was taken into account by dividing them into four sections (two sections per window). The characteristic length of grouped elements required for analysis is about 20 to 50 cm.
- The capacities were analytically evaluated, taking into account the adjacent conductors dispositions and neglecting the capacitances of conductors located in different disks.
- The modeling results show some differences versus the measured values in the laboratory test (Table 4.16), which can be attributed to the simplifying assumptions and to the axisymmetric modeling.

- The simplified scheme ATP-EMTP can be used to identify the influence of autotransformer constructive parameters at a certain level and form of applied lightning surges.
- Optimization of solutions in 3-D numerical simulations were searched to reduce the solving time and to increase the accuracy. It's known that, if necessary, the computer's operating system supplements the random access memory (RAM, physical memory) by additional memory located on hard disk, which drastically slows down the program running. Consequently, the author has taken over the PC memory management through a configuration file, specific to ANSYS. Thus, the amount of additional memory could be minimized by its differentiated allocation along the phases of pre-processing, processing and post-processing.
- Also, based on nodes number used by each formulation, the solving time could be evaluated under assumptions of an unlimited physical memory. The results presented in Table 4.9 show that using additional memory in the range (1.5-3.0) GB, increases the solving time of (10-24) times compared to the ideal case.
- The large multiple numerical simulations have confirmed that the solutions are faster obtained, as the computer physical memory is more important, which minimizes the amount of additional memory required from the hard disk.

Chapter V concerns transient phenomena taking place in a system of two solid rectangular parallel bus bars, to the step signals application of current and voltage. The transient magnetic field problem for infinitely high bars is completely analytically solved [161], considering a zero magnetic field on the outer surfaces of both bars. New analytical results [41] were obtained for finite height but large enough bars, maintaining the assumption of one-dimensional magnetic field inside the bars, constantly distributed on the height, but considering a nonzero magnetic field on the outer sides. The ratio η, of the fields in the middle of the two sides of the high bar, was also held constant.

The author has numerically simulated the penetration process of electric and magnetic fields into the system bar (Fig. 5.2) using 2-D FEM. The simulation results were compared with analytical ones and combined with them to improve the effects of simplified assumptions. The contributions to the study of this transient phenomenon are given below:

- The transient regimes established in the system of two solid rectangular parallel very high bars (h/b = 30) (Fig. 5.2), to the step signal application of current and voltage, was simulated using 2-D FLUX [172] and FEMM [175] programs. Being an open boundary problem, the FLUX facilities were used for this purpose, by bordering the bars system with so-called *infinite box*, respectively, by asymptotic boundary conditions available in FEMM.
- To increase the accuracy, the spatial and temporal mesh have been refined in areas with large quantities variations, i.e. along the edges of the bars and especially around the peaks and to towards the beginning of the transient process. A major influence has a rate of change of elements size in the mesh. Thus, the step time was increased in steps, keeping it constant on small time intervals, aiming to have jumps no more than 2-2.5 times to junctions of uniform intervals.
- The evolution of the ratio η along the transient process was numerically determined using FLUX to the step signal application of current and voltage. In both cases there was observed a negative slope of the numerical curves on the first two decades (Fig. 5.15, 5.22), explained by inevitably rough temporal mesh on these sections.
- To investigate the value of η ratio at absolute initial moment (t = 0) (η_0), static simulations were performed in FEMM program. The expulsion effect of the field lines from

conductor domain in this moment was obtained by a trick involving the approximate cancellation of its relative permeability.

- The FEMM numerical simulations at the moment $t = 0$ led to values very close to the minimum of numerical curves obtained by FLUX, indicating the moments from when the transient simulation in the FLUX can be taken into account.
- The FEMM investigation for extremely thin bars ($b/a = 0.01$) (Fig. 5.2) validates enough well the results for η_0 obtained by conformal mapping method (CMM) [48] for $b/a = 0$ configuration.
- Large differences were found compared to analytical values of η_0 [41] (Fig. 5.6, 5.15, 5.22) indicating that the assumptions under which the ratio was analytically derived at time $t = 0$, are very approximate.
- However, in the stationary regime, the numerical simulations lead to the same results as the analytical calculations, based on testing of a large variety of geometric configurations (Fig. 5.7, 5.8).
- The analytical determination of the tangential and longitudinal components of magnetic field [41] was based on the use of a constant ratio η, equal to its value in stationary regime η_{st}. Even under this assumption, the comparison between numerical and analytical curves for different moments of the transient process shows good agreement, excepting the external sides of the bars (Fig. 5.16, 5.18, 5.23, 5.25).
- The time variation of electric and magnetic fields on the periphery of the bar, numerically determined (points A and B, Fig. 5.1) confirms the agreements with analytical results, excepting the first decades, where the errors of numerical method are visible (Fig. 5.20, 5.21, 5.27, 5.28).
- The author has proposed a mixed analytical-numerical solution (Fig. 5.17, 5.19, 5.24, 5.26) based on analytical equations [41] with the use of a variable ratio η, given by the numerical simulation in FLUX (Fig. 5.15, 5.22).
- The numerical simulations in FEMM had continued at $t = 0$ moment, for different geometric configurations, validating results of numerical conformal mapping method [49] using the Schwartz-Christoffel (SC) module of MATLAB software and also validating new very simple analytical formulas for η_0 ratio (5.27) and for its average (5.28) [49], for small thickness bars, using the coefficient $(h+b)/a$ used by Dwight for determining the electrodynamics forces between the bars.
- The average of ratio η_b of tangential components of magnetic fields at points C and A (η_{bmed}) (Fig. 5.2) was subject of the same type of numerical investigations. It was validated the SC evaluation and analytical expression (5.29) [49], observing a low dependence of the ratio h/a.
- Automation of calculation in FEMM program was obtained by running the command files (*scripting files*), created using parametric language LUA [176] for pre-processing, processing and post-processing, which does not exclude the interactive work.

- In **Chapter VI** were numerically determined by 2-D FEM the transient parameters of the system of solid rectangular parallel very high bars ($h/b = 30$) (Fig. 5.2) and based on analytical relationships between them, established by *the theory of transient parameters of linear electric circuits* (TPTLEC) [140], the ones of them were derived from the others, making comments on certain founded irregularities. The author's contributions in transient parameters evaluation are listed below:
- The 2D simulations using the FLUX program described in chapter V on the transient process of the bars system at the application of step or ramp signals of current and voltage, had allowed the determination of three transient parameters: *transient resistance*,

directly deduced from the numerical value of the applied voltage (6.100), (6.105), *transient conductance*, directly deducted from the numerical value of the injected current (6.100), (6105) and *transient inductance*, directly offered by FLUX, based on the classical definition of total magnetic flux (6.96) (6.97) (6.98).

- The analytical relationships between the parameters established by TPTLEC [140] had allowed the calculation of *transient inductance* from transient resistance (6.103), (6.107) containing in its expression the inductance in stationary regime L_{st} and the calculation of *transient capacitance* from transient conductance, containing in its expression the capacitance in stationary regime C_{st} (6.115) or initial capacitance C_{in} (6.120).
- The determination of initial capacitance C_{in} was made in the particular feeding regime of ramp voltage application, for which the TPTLEC [140] provides a relationship witch contains the current and its derivative with respect the time (6.118), (6.117). Given that C_{in} is a constant quantity, its value should result the same, no matter of the moment of its evaluation. The author has proposed a formula for C_{in} (6.119) that makes the average of 234 values, corresponding to the moments describing the analyzed transient process, covering ten decades.
- The stationary capacitance C_{st} was considered equal to the transient capacitance at ramp voltage application, calculated at the last moment, corresponding of ten time constants.
- The stationary inductance L_{st} was evaluated in magneto static regime, verifying very well the numerical value of transient inductance, directly given by FLUX and calculated at the last moment.
- Mutually, based on analytical formulas of TPTLEC [140], from numerical value of the transient inductance, directly offered by FLUX (total inductance), was calculated transient resistance (6.101), (6.105).
- Following the same methodology as for C_{in}, the initial inductance L_{in} was also determined in particular feeding regime of ramp current injection, for which the TPTLEC [140] provides a relationship witch contains the voltage and its derivative with respect the time (6.108), (6.105). Given that L_{in} is a constant quantity, its value should result the same, no matter of the moment of its evaluation. The author has proposed a formula for L_{in} (6.109) that makes the average of 234 values, corresponding to the moments describing the analyzed transient process. The L_{in} value was very precisely validated by FEMM static simulation (Chapter V).
- The comparisons between the numerical and analytical-numerical results of the transient parameters point out some differences that may have several causes. Thus, the numerical simulation of the beginning of transient regime is strongly affected by the temporal mesh inevitably rough in the first decades. The errors in the middle decades can be attributed to the different ways of definition of *transient inductance*. The FLUX program [172] evaluate this parameter by the classical definition using the total magnetic flux (6.96), (6.97), while TPTLEC [140] uses an equivalent flux, linked to inductance by a convolution product (6.78). Other sources of error may also be application of derivative operators on interpolated numerical signal. A more fine mesh could improve the accuracy of the results.
- The features of the solid conductor versus the ideal filiform conductor were pointed out by comparing the evolutions of terminals quantities in feeding regime of ramp signals of current and voltage.
- The author has built a graphic animation that simulates the penetration of electric and magnetic fields into the rectangular bars system at current step injection.

REFERENCES

[1] Ahagon, A., *Comparison of various kinds of edge elements for electromagnetic field analysis*, IEEE Transaction on Magnetics, Vol. 32, No. 3, May 1996, pp. 898-901;

[2] Andea, P., *Electromagneții*, Helicon Publishing House, Timişoara, 1993;

[3] *ANSYS Release 9.0 Documentation*, 2004;

[4] Ardeleanu, M., *Metode de studiu al câmpurilor electrice şi magnetice asociate cablurilor subterane*, PhD. Report, University of Craiova, 2003;

[5] Azzouz, Z.E., *Modélisation 3D d'un transformateur de puissances. Etude de son comportement à haute fréquence*, PhD. Thesis, Institut National Polytechnique de Grenoble (INPG), Laboratoire d'Electrotechnique de Grenoble (LEG), 1992;

[6] Bardi, I., *Nodal and edge element analysis of inhomogeneously loaded 3-D cavities*, IEEE Transaction on Magnetics, Vol. 28, No. 2, March 1992, pp. 1142-1145;

[7] Barré, O., Broche, P., Hecquet, M., *Experimental validation of magnetic and electric local force formulations associated to energy principle*, Vol. 42, No. 4, April 2006, pp. 1475-1478;

[8] Bateman, H., Erdelyi, A., *Higher Transcendental Function*, Vol. 2, Mc. Graw-Hill, New York, 1953;

[9] Benhama, A., Williamson, A.C., Reece, A.B.J., *Computation of electromagnetic forces from finite element field solutions*, Third International Conference on Computation in Electromagnetics, April 10-12, 1996, pp. 247-252;

[10] Benhama, A., Williamson, A.C., Reece, A.B.J., *Force and torque computation from 2-D and 3-D finite element field solutions*, Electric Power Applications, IEE Proceedings, Vol. 146, No. 1, January 1999, pp. 25-31;

[11] Benhama, A., Williamson, A.C., Reece, A.B.J., *Virtual work approach to the computation of magnetic force distribution from finite element field solution*, Electric Power Applications, IEE Proceedings, Vol. 147, No. 6, November 2000, pp. 437-442;

[12] Berbente, C., Mitran, S, Zancu, S., *Metode numerice*, Tehnica Publishing House, Bucureşti, 1997;

[13] Binns, K.J., Lawrenson, P.J., *Analysis and computation of electric and magnetic field problems*, Pergamon Press, Oxford, 1963;

[14] Biro, O., Preis, *On the use of the magnetic vector potential in the finite element analysis of three-dimensional eddy currents*, IEEE Transaction on Magnetics, Vol. 25, No. 4, July 1989, pp. 3145-3159;

[15] Biro, O., Preis, K., Richter, K., *On the use of the magnetic vector potential in the nodal and edge finite element analysis of the 3-D magnetostatic problems*, IEEE Transaction on Magnetics, Vol. 32, No. 3, 1996, pp. 651-654;

[16] Blache, F., *Modélisations électronique et électromagnétique d'un transformateur haute fréquence à circuit magnétique en fonte*, PhD. Thesis, Institut National Polytechnique de Grenoble (INPG), Laboratoire d'Electrotechnique de Grenoble (LEG), 1995 ;

[17] Bossavit, A., *A rationale for Edge-elements in 3-D fields computations*, IEEE Transaction on Magnetics, Vol. 24, No. 1, January 1988, pp. 74-79;

[18] Burden, R.L., Faires, D.J., *Numerical Analyses - third edition*, PWS-KENT Publishing Company, Boston, 1985;

[19] Carron, G., *Contribution à la modelisation des phenomenes magnetodynamiques en trois dimensions*, PhD. Thesis, Institut National Polytechnique de Grenoble (INPG), Laboratoire d'Electrotechnique de Grenoble (LEG), 1990;

[20] Champaney, L., *Méthodes d'Approximation de Solution pour les Problèmes de Physique*, Course, University of Versailles St-Quentin in Yvelines, 2005;

[21] Chari, M.V.K., Bedrosia, G., D'Angelo, J., Konrad, A., *Finite element application in electrical engineering*, IEEE Transaction on Magnetics, Vol. 29, No. 2, March 1993, pp. 1306-1314;

[22] Chen, S.X., Low, T.S., Mah, Y.A, Jabbar, M.A., *Super convergence theory and its application to precision force calculation*, IEEE Transaction on Magnetics, Vol. 32, No. 5, September 1996, pp. 4275-4277;

[23] Choi, H.S., Park, I.H., Lee, S.H., *Concept of virtual air gap and its applications for force calculation*, IEEE Transaction on Magnetics, Vol. 42, No. 4, April 2006, pp. 663-666;

[24] Choi, H.S., Lee, S.H., Park, I., *Implementation of virtual air-gap for Maxwell stress tensor*, 12-th Biennial IEEE Conference on Electromagnetic Field Computation, June 2006, pp. 401-401;

[25] Cira, O., *Lecții de MathCad*, Albastra Publishing House, Cluj-Napoca, 2000;

[26] Cividjian, G.A., Degeratu, P., Cernian, O., *The calculation of the dimensions for an electromagnet with T-armature*, Proceedings of the XIII-th Conference on Design automation, pp. 495-501, San Francisco, California, United States, June 28-30, 1976;

[27] Cividjian, G., Degeratu, P., Cernian, O., *Dimensionarea electromagneților cu armatură în T*, (*Dimensioning the T-armature electromagnets*), The XII-th Technical Scientific Session of ICPE, reff. 152/G, pp. 3-20, November 4-6, Bucureşti, 1976;

[28] Cividjian, G., Radulian, G., *Inductanța electromagneților cu armatură în T*, (*Inductance of the T-armture electromagnets*), The XII-th Technical Scientific Session of ICPE, ref. 185/A, pp. 1-10, November 4-6, Bucureşti, 1976;

[29] Cividjian, G.A., *Aparate electrice. Partea I*, University of Craiova publishing House, 1979;

[30] Cividjian, G.A., Popa, I., Leoveanu Maria, *Forța de atracție la electromagneții cu armatură în T* (*Force of T-armature electromagnets*), National Conference on Electricity and Energy, CNEE '82, Vol. 9, pp. 65-70, Timişoara, September 17-18, 1982;

[31] Cividjian, G.A., Popa, I., Leoveanu, Maria, *Programs for the dimensioning of U, E and T - electromagnets*, The IV-th National Conference on Electrical Drives, pp. 69-74, Craiova, 1984;

[32] Cividjian, G.A., *Stepennaia approksimatia granicinyh uslovií pri rescete poleí razdeleniem peremennyh*, (*Power approximation of boundary conditions at field calculation by variables separation*), The III-rd International Symposium on Theoretical Electricity, pp. 128-129, Moscow, 1985;

[33] Cividjian, G.A., *Vlianie glubiny paza i nasyscenia na koeffitient vozdushnogo zazora*, (*Influence of the slot depth and of the saturation on the Carter coefficient*), Elektrichestvo, No.6, pp. 59-61, ISSN 0013-5380, 1986;

[34] Cividjian, G.A., *Aparate electrice. Izolaţie şi arc*, Avrameanca Publishing House, Craiova, 1996;

[35] Cividjian, G.A. ş.a., *Power approximation of boundary conditions*, Seconde Conférence Européenne sur les Méthodes Numériques en Electromagnetisme, NUMELEC ’97, March 19-21, pp. 252-253, Lyon, 1997;

[36] Cividjian, G.A. ş.a., *Inductance of a plunger-type magnet*, IEEE Transaction on Magnetics, Vol. 34, No. 5, pp. 3695-3688, September, 1998;

[37] Cividjian, G.A., Cividjian, A.G., Silvis-Cividjian, N.G., *Some formulas for two-dimensional permeances*, IEEE Transaction on Magnetics, Vol. 36, No. 5, September 2000, pp. 3754-3758;

[38] Cividjian, G.A., Cividjian, A.G., Silvis-Cividjian, N.G., *Two formulas for 2D permeances,* COMPEL - International journal for computation and mathematics in electrical and electronic engineering, Vol. 19, No. 2, 2000, pp. 260-267, ISSN 0332-1649;

[39] Cividjian, G.A., Pascu, Ileana, Bunescu, A., Matei, D., M., **Dolan, A.,** *Experimental study of the resistance of flat Cu-W contacts*, XII-th International Symposium on Electrical Apparatus and Technologies - SIELA 2001, Vol. I, pp. 58-65, Plovdiv, Bulgaria, May 31 – June 1-st, 2001;

[40] Cividjian, G.A., **Dolan, A.,** Climov, V., Canakoglu, A., I., *Inductance of plunger -type electromagnet*, International Conference on Applied and Theoretical Electricity - ICATE 2002, pp. 193-198, Băile Herculane, Romania, October 17-19, 2002;

[41] Cividjian, G.A., *Current distribution in rectangular busbars*, Revue Roumaine des Sciences Electrotechnique et Energétiques, Vol. 48, No. 2/3, pp. 313–320, Bucureşti, 2003;

[42] Cividjian, G.A., *Current distribution in variable section fuses*, Seventh International Conference on Electrical Fuses and their Applications - ICEFA, Gdansk-Jurata, Polonia, September 8-10, 2003, pp. 194-199, ISBN 83-88829-76-9;

[43] Cividjian, G.A., Călin, G., Popa, D., **Dolan, A.**, *Modeling lightning surges in power transformer*, The Second International Symposium on High Voltage and High Power Tests, Measurements and Quantification of Electrical Power Equipment - SIMC-EE 2004, Băile Herculane, October 13-15, 2004, CD;

[44] Cividjian, G.A., **Dolan, A**., Păduraru, N., *Inductance of Cylindrical Coil*, Serbian Journal of Electrical Engineering, Vol. 1, No.2, pp. 143-151, Technical Faculty of Cacak, Serbia and Montenegro, June, 2004, ISSN 1451-4869;

[45] Cividjian, G.A., Călin, G., Popa, D., **Dolan, A.,** *Impedance voltage of power multi-winding autotransformer*, XIV-th International Symposium on Electrical Apparatus and Technologies - SIELA 2005, Vol. I, pp. 39-44, Plovdiv, Bulgaria, June 2-3, 2005, ISBN 954-90209-4-0;

[46] Cividjian, G.A., *Some formulas for partial capacitances*, International PhD Seminar - Numerical Field Computation and Optimization in Electrical Engineering, pp. 45-54, Ohrid, Macedonia, September 20-25, 2005;

[47] Cividjian, G.A., Cividjian, A.G., *Constriction and corner permeances for finite domains*, IEEE Transaction on Magnetics, Vol. 42, No. 12, December 2006, pp. 3825-3831;

[48] Cividjian, G.A., *Initial magnetic field distribution around high rectangular busbars*, Simpozionul Naţional de Electrotehnică Teoretică - SNET ’07, October 12-14, Bucureşti, 2007 (Unpublished);

[49] Cividjian, G.A., *Initial magnetic field distribution around rectangular busbars*, Annals of University of Craiova, Series: Electrical Engineering, No. 32, pp. 68-71, 2008, Universitaria Publishing House, ISSN 1842-4805;

[50] Cividjian, G.A., *Permeance of fringing flux*, IEEE Transaction on Magnetics, Vol. 45, No. 2, February 2009, pp. 694-700;

[51] Cividjian, G.A., **Dolan, A.,** Yatchev, I., Hinov, K., *On the tractive force of plunger-type magnet,* XVI-th International Symposium on Electrical Apparatus and Technologies - SIELA 2009, Vol. I, pp. 63-70, Burgas, Bulgaria, June 4-6, 2009, ISBN 978-954-323-530-8;

[52] Coulomb, J.L., *Finite element three dimensional magnetic field computation*, IEEE Transaction on Magnetics, Vol. MAG-17, No. 6, November 1981, pp. 3241-3246;

[53] Coulomb, J.L., *A methodology for the determination of global electromagnetical quantities from a finite element analysis and its application*, IEEE Transaction on Magnetics, Vol. MAG-19, No. 6, November 1983, pp. 2514-2519;

[54] Coulomb, J.L., Meunier, G., *Finite element implementation of virtual work principle for magnetic or electric force and torque computation*, IEEE Transaction on Magnetics, Vol. MAG-20, No. 5, September 1984, pp. 1894-1896;

[55] Coulomb, J.L., Meunier, G., Sabonnadiere, J.C., *Energy methods for the evaluation of global quantities and integral parameters in a finite elements analysis of electromagnetic devices*, IEEE Transaction on Magnetics, Vol. MAG-21, No. 5, September 1985, pp. 1817-1822;

[56] De Medeiros, L.H.A., *Méthodes de calcul des forces électromagnétiques. Application au calcul des distributions de forces sur les aimants permanents,* PhD. Thesis, Institut National Polytechnique de Grenoble (INPG), Laboratoire d’Electrotechnique de Grenoble (LEG), 1998;

[57] Dedule, J.M, *Contribution à la modélisation bidimensionnelle et tridimensionnelle des phénomènes d'anisotropie dans transformateurs triphasés*, PhD. Thesis, Institut National Polytechnique de Grenoble (INPG), Laboratoire d'Electrotechnique de Grenoble (LEG), 1990;

[58] Demerdash, N.A., Fouad, F.A., Nehl, T.W., Mohamed, O.A., *Three dimensional finite element vector potential formulation of magnetic fields in electrical apparatus*, IEEE Transaction on Power Apparatus and Systems, Vol. PAS-100, No. 8, August 1981, pp. 4104-4111;

[59] Démidovitch, B., Maron, I., *Éléments de calcul numérique*, Mir Publishing House, Moscow, 1979;

[60] Demski, W., Szymanski, G., *Comparison of the force computation using the vector and scalar potential for 3-D*, IEEE Transaction on Magnetics, Vol. 33, No. 2, March 1997, pp. 1231-1234;

[61] **Dolan, A.,** Yatchev, I., Hinov, K., *Static force characteristics of a plunger type electromagnet*, International PhD Seminar - Numerical Field Computation and Optimization in Electrical Engineering, Ohrid, Macedonia, September 20-25, 2005, pp. 67-71;

[62] **Dolan, A.,** *Metode numerice de calcul al câmpurilor electrice, magnetice şi termice*, PhD. Report, University of Craiova, May 2006;

[63] **Dolan, A.,** *Softuri comerciale pentru modelarea câmpurilor şi a regimurilor tranzitorii*, PhD. Report, University of Craiova, May 2006;

[64] **Dolan, A**., Yatchev, I., Hinov, K., *Comparison of different formulations and techniques for 3D static force computation of a T-shaped electromagnet,* International PhD Seminar - Computational Electromagnetics and Technical Applications, pp. 73-77, Banja Luka, Bosnia and Herzegovina, August 28 - September 1-st, 2006, ISBN 99938-793-5-5;

[65] **Dolan, A.**, Cividjian G.A., Yatchev, I., Călin, G., Popa, D., *Three dimensional numerical solution for impedance voltage of power multi-winding autotransformer,* Annals of University of Craiova Craiova, Series: Electrical Engineering, No. 30, pp. 326-329, 2006, Universitaria Publishing House, ISSN 1842-4805;

[66] **Dolan, A.**, *Simulation de dispositifs électrotechniques par FLUX 2D-3D - Transformateur triphasé,* Stage Report, Grenoble Electrical Engineering Laboratory (G2Elab), French, March 2007;

[67] **Dolan, A.,** Cividjian, G.A., Yatchev, I., Calin, G., Popa, D., *Different formulations for power multi-winding autotransformer impedance voltage evaluation,* XV-th International Symposium on Electrical Apparatus and Technologies - SIELA 2007, Vol. II, pp. 15-24, Plovdiv, Bulgaria, May 31 - June 1-st, 2007, ISBN 978-954-9726-01-5;

[68] **Dolan, A.,** *Parametrii tranzitorii ai circuitelor electrice liniare*, PhD. Report, University of Craiova, September 2007;

[69] **Dolan, A.**, Cividjian, G.A., *Numerical solutions for transient electromagnetic field in rectangular bus bars,* National Symposium of Theoretical Engineering - SNET '07, October 12-14, pp. 406-411, Bucureşti, 2007;

[70] **Dolan, A.,** Cividjian G.A., *Numerical determination of rectangular busbars transient parameters,* Annals of University of Craiova, Series: Electrical Engineering, No. 32, pp. 210-215, 2008, Universitaria Publishing House, ISSN 1842-4805;

[71] Du, I.M., Xia, P.C., Xiao, L.Y., *Calculating magnetic force of permanent magnet using Maxwell stress method,* IEEE Transaction on Applied Superconductivity, Vol. 10, No. 1, March 2000, pp. 1392-1394;

[72] Dufour, F., *Développement de la méthode des éléments finis avec des points d'intégration lagrangiens: application à la géomécanique***,** PhD. Thesis, Centrale School of Nantes & University of Nantes, 2002;

[73] Ebâncă, D., *Metode de calcul numeric,* Sitech Publishing House, Craiova, 1994;

[74] *FEMM, Version 3.4, User's Manual,* 2005;

[75] *FLUX 9.3.2, Guide d'utilisation,* 2006;

[76] Freeman, E.M., Ashen, E.M., *Force calculation in magnetic field problems using virtual work with only one solution,* Sixth International Conference on Electrical Machines and Drives, September 8-10, 1993, pp. 318-322;

[77] Giannacopoulos, D., McFee, S., *An experimental study of superconvergence phenomena in finite element magnetics,* IEEE Transaction on Magnetics, Vol. 33, No. 5, September 1997, pp. 4137-4139;

[78] Golias, N.A., Tsiboukis, T.D., *Magnetostatics with edge elements: a numerical investigation in the choice of the tree*, IEEE Transaction on Magnetics, Vol. 30, No. 5, September 1994, pp. 1488-1491;

[79] Guerin, C., *Détermination des pertes par courants de Foucault dans les cuves de transformateurs. Modélisation de régions minces et prise en compte de la saturations des matériaux magnétiques en regime harmoniques*, PhD. Thesis, Institut National Polytechnique de Grenoble (INPG), Laboratoire d'Electrotechnique de Grenoble (LEG), 1994;

[80] Guillen, M., Poittevin, J., Aucourt, Ch., *Modélisation numérique et essais: complémentarité de deux moyens d'investigation pour la haute tension*, Revue de l'Electricité et de l'Electronique (REE), No. 10, November, pp. 15-20, 1996;

[81] Guşă, M.D., *Regimuri tranzitorii în reţelele electrice*, „Gh. Asachi" Publishing House, Iaşi, 2002;

[82] Gyimesi, M., Lavers, D., *Generalized potential formulation for 3-D magnetostatic problems*, IEEE Transaction on Magnetics, Vol. 28, No. 4, July 1992, pp. 1924-1929;

[83] Gyimesi, M., Lavers, D., Pawlak, T., Ostergaard, D., *Application of the general potential formulation*, IEEE Transaction on Magnetics, Vol. 29, No. 2, March 1993, pp. 1345-1347;

[84] Gyimesi, M., Lavers, D., Pawlak, T., Ostergaard, D., *Biot-Savart integration for bars and arcs*, IEEE Transaction on Magnetics, Vol. 29, No. 6, November 1993, pp. 2389-2391;

[85] Gyimesi, M., Avdeev, I., Ostergaard, D., *Finite Element Simulation of Micro Electro Mechanical Systems* (*MEMS*) *by Strongly Coupled Electro Mechanical Transducers*, IEEE Transactions on Magnetics, Vol. 40, No. 2, pp. 557–560, 2004;

[86] Hebrin, R., *Cours d'analyse numérique 2004-2005*, Course, Master in Mathématics, University of Aix Marseille 1, 2004;

[87] Hennenberger, G., *Force calculation with analytical accuracy in the finite element based computational magnetostatics*, IEEE Transaction on Magnetics, Vol. 27, No. 5, September 1991, pp. 4254-4257;

[88] Heydari, H., Pedramrazi, S.H., Faghihi, F., *The effects of windings current density values on leakage reactance in a 25 kA current injection transformer*, The 7-th International Power Engineering Conference - IPEC 2005, November 29 - December 02, 2005, pp. 648-652;

[89] International Electrotechnical Commission (IEC), *Multi-Lingual Dictionary of Electricity, Electronics, and Telecommunications*, Vol. 1, Elsevier, Amsterdam, New-York, Tokyo, Oxford, 1992;

[90] Imhoff, J.F, *Modélisation magnétique et mécanique des machines électriques par la méthode des éléments finis*, PhD. Thesis, Institut National Polytechnique de Grenoble (INPG), Laboratoire d'Electrotechnique de Grenoble (LEG), 1989;

[91] International Compumag Society (ICS), Testing Electromagnetic Analysis Methods (TEAM), *Problem 13*;

[92] International Compumag Society (ICS), Testing Electromagnetic Analysis Methods (TEAM), *Problem 20*;

[93] Ioan, D., Munteanu, Irina, Ionescu, B., Popescu, M., Popa, R., Lăzărescu, M., Ciuprina, Gabriela, *Metode numerice în ingineria electrică*, Matrix Rom Publishing House, Bucureşti, 1998;

[94] Ito, M., Tajima, F., Kanazawa, H., *Evaluation of force calculation methods*, IEEE Transaction on Magnetics, Vol. 26, No. 2, March 1990, pp. 1035-1038;

[95] Ivanov, Virginia, *Aplicaţii în Mathcad şi Matlab*, Vol. I, Universitaria Publishing House, Craiova, 2008;

[96] Joan, M., *Modélisations des paramètres R et L de matériels électriques bobinés par la méthode des éléments finis 3D*, PhD. Thesis, Institut National Polytechnique de Grenoble (INPG), Laboratoire d'Electrotechnique de Grenoble (LEG), 2004 ;

[97] Kabashima, T., Kawahara, A., Goto, T., *Force calculation using magnetizing currents*, IEEE Transaction on Magnetics, Vol. 24, No. 1, January 1988, pp. 451-454;

[98] Karsay, K., Kerenyi, D., Kiss, L., *Large Power Transformers*, Akademiai Kiado, Budapest, 1987;

[99] Kashtiban, A.M., Vahedi, A., Halvaei, A., *Investigation of winding type effect on leakage flux of single phase shell type transformer using FEM*, Proceedings of the Eighth International Conference on Electrical Machines and Systems - ICEMS 2005, Vol. 3, 29 September, 2005, pp. 1755-1758;

[100] Kanai, Y., Abe, T., Sengoku, M., Iijiama, T., Iizuka, M., Mukasa, K., *New formulation of finite-element method with gauge condition for three-dimensional magnetic field analysis*, IEEE Transaction on Magnetics, Vol. MAG-24, No. 6, November 1988, pp. 3123-3125;

[101] Kanai, Y., Abe, T., Sengocu, M., Iijima, T., Iizuka, M., Mukasa, K., *Further discussion on magnetic vector potential finite-element formulation for three-dimensional magnetostatic field analysis*, IEEE Transaction on Magnetics, Vol. 26, No. 2, March 1990, pp. 411-414;

[102] Kim, D.H., Lowter, D.A., Sykulski, J.K., *Efficient force calculation based on continuum sensitivity analysis*, IEEE Transaction on Magnetics, Vol. 41, No. 5, May 2005, pp. 1404-1407;

[103] Kladas, A.G., Papadopoulos, M.P., Tegopoulos, J.A., *Leakage flux and force calculation on power transformer windings under short-circuit: 2-D and 3-D models based on the theory of images and the finite element method compared to measurements*, IEEE Transaction on Magnetics, Vol. 30, No. 5, September 1994, pp. 3487-3490;

[104] Komeza, K., Pelikant, A., Tegopoulos, J., Wiak, S., *Comparative computation of forces and torques of electromagnetic devices by means of different formulae*, IEEE Transaction on Magnetics, Vol. 30, No. 5, September 1994, pp. 3475-3478;

[105] Kostensko, M., Piotrovski, L., *Electrical machines* (In French), Mir, Moscow, 1976 ;

[106] Krylov, V.I., Skoblya, N.S., *Handbook for numerical Laplace inversion* (In Rush), Nauka I Tehnika, pp. 18 and 53, Minsk, 1968;

[107] Lefevre, A., Miegeville, L., Fouladgar, J., Olivier, G., *3-D computation of transformers overheating under nonlinear loads*, IEEE Transaction on Magnetics, Vol. 41, No. 5, May 2005, pp. 1564-1567;

[108] Lefevre, A., *Contributions à la modélisation électrique, électromagnétique et thermique des transformateurs - Application à l'étude de l'échauffement sur charges non linéaires*, PhD. Thesis, University of Nantes, 2006 ;

[109] Longfu, L., Ziya, W., Tiaosheng, T., *The method solving short-circuit impedance between two interleave windings in the multi-winding core-type transformer with finite element method*, Proceedings of the Fifth International Conference on Electrical Machines and Systems - ICEMS 2001, Vol. 1, August 18-20, 2001, Shenyang, China, pp. 254-256;

[110] Lowther, D.A., *The implications of three-dimensional mesh generation on the calculation of mechanical forces in magnetic devices*, IEEE Transaction on Magnetics, Vol. 26, No. 5, September 1990, pp. 2777-2779;

[111] Marinescu, A., *Transformer behaviour at switching overvoltages* (In romanian), Tehnica Publishing House, Bucureşti, 1988;

[112] Marinescu, A., Călin, Gh., *HV Power Auto-Transformers Protected for Internal Overvoltages*, Proceedings of the 8-th International Conference on Optimization of Electrical and Electronic Equipments, May 16-17, Braşov, 2002;

[113] Markovici, J., *Asupra regimului permanent periodic în conductoare masive*, Annals of University of Craiova - Mathematics, Physics, Chemistry, Electrical Engineering, Fifth Series, No. 2, pp. 205-208, 1973;

[114] Maiergoyz, I.D., Chari, M.V.K., D'Angelo, J., *A new scalar potential formulation for three dimensional magnetostatic problems*, IEEE Transaction on Magnetics, Vol. MAG-23, No. 6, November 1987, pp. 3889-3894;

[115] Meunier, G., *Electromagnétisme et problèmes couplés*, Hermès Science Publishing House, Paris, 2002;

[116] McFee, S., Lowther, D.A., *Towards accurate and consistent force calculation in finite element based computational magnetostatic*, IEEE Transaction on Magnetics, Vol. MAG-23, No. 5, September 1987, pp. 3771-3773;

[117] McFee, S., Webb, J.P., Lowther, D.A., *A tunable volume integration formulation for force calculation in finite element based computational magnetostatic*, IEEE Transaction on Magnetics, Vol. 24, No. 1, January 1988, pp. 439-442;

[118] Mizia, J., Adamiak, K., Eastham, A.R., Dawson, G.E, *Finite element force calculation: comparison of methods for electric machines*, IEEE Transaction on Magnetics, Vol. 24, No. 1, January 1988, pp. 447-450;

[119] Mocanu, C.I., *Teoria câmpului electromagnetic*, EDP, Bucureşti, 1981;

[120] Morega, M., A., *Elemente de modelare numerică pentru probleme la limită*, Polytechnic Institute of Bucharest Publishing House, 1997;

[121] Morisue, T., *Infinitely many formulation using the magnetic vector potential with the Coulomb gauge for the 3-D field calculations*, IEEE Transaction on Magnetics, Vol. 26, No. 2, March 1990, pp. 715-718;

[122] Müller, W., *Comparison of different methods of force calculation*, IEEE Transaction on Magnetics, Vol. 26, No. 2, March 1990, pp. 1058-1061;

[123] Nakata, T., Takahashi, N., Fujiwara, K., Imai, T., Muramatsu, K., *Comparison of various methods of analysis and finite elements in 3-D magnetic field analysis*, IEEE Transaction on Magnetics, Vol. 27, No. 5, September 1991, pp. 4073-4076;

[124] Nehl, T.W., *Accuracy of force calculations using first order tetrahedra for electromagnetic devices with small air gaps*, IEEE Transaction on Magnetics, Vol. 27, No. 5, September 1991, pp. 4250-4253;

[125] Nens, E., *Contribution à la modélisation des structures symétriques en électromagnétisme*, PhD. Thesis, Institut National Polytechnique de Grenoble (INPG), Laboratoire d'Electrotechnique de Grenoble (LEG), Faculté Polytechnique de Mons, 2002;

[126] Nicolaide, A., *Bazele fizice ale electrotehnicii*, Vol. I-II, Scrisul Românesc Publishing House, Craiova, 1983;

[127] Ngnegueu, T., *Contribution à la modélisation mathématique et informatique des pertes supplémentaires dans les transformateurs de puissance de type cuirasse*, PhD. Thesis, Institut National Polytechnique de Grenoble (INPG), Laboratoire d'Electrotechnique de Grenoble (LEG), 1989;

[128] Ohdachi, Y., Kawase, Y., Tainaka, T., Yamaguchi, T., *Load characteristics analysis of coupling transformer using 3-D finite element method with edge elements*, IEEE Transaction on Magnetics, Vol. 30, No. 5, September 1994, pp. 3721-3724;

[129] Olaru, D., *Metode numerice - Aplicaţii implementate în MathCad*, Polytechnic Institute of Bucharest Publishing House, 1997, 2002;

[130] Park, Y.G., Kim, H., Hahn, S., *An adaptive finite element method for magnetostatic force computation*, IEEE Transaction on Magnetics, Vol. 26, No. 2, March 1990, pp. 1031-1034;

[131] Păltineanu, G., Matei, P., Trandafir, R., *Bazele analizei numerice*, Printech Publishing House, Bucureşti, 2000;

[132] Petrov, G.N., *Электрические машины ч. 1, Трансформаторы*, ГЭИ, Москва, 1956;

[133] Popa, I., *Modélisation numérique du transfert thermique - Méthode des volumes finis*, Universitaria Publishing House, Craiova, 2002;

[134] Prasad, K.M., Davey, K.R., *A boundary element analysis of Team Problem no. 20: Static force calculation*, 4-th International TEAM Workshop, November 1993;

[135] Preda, M, Markovici, J., Topan, D, *Asupra imitanţelor parametrilor tranzitorii pentru circuitele nefiliforme, a relaţiilor dintre acestea şi parametrii de regim nesinusoidal*, EEA – Electrotehnica, Year 23, No. 1, pp. 15-22, 1975;

[136] Preda, M., ş.a., *Bazele electrotehnicii*, Vol. I, EDP, Bucureşti, 1980;

[137] Preis, K., Bardi, I., Biro, O., Magele, C., Renhart, W., Richter, K.R., Vrisk, G., *Numerical analysis of 3-D magnetostatic fields*, IEEE Transaction on Magnetics, Vol. 27, No. 5, September 1991, pp. 3798-3803;

[138] Preis, K., Bardi, I., Magele, C., Vrisk, G., Richter, K.R., *Different finite element formulations of 3-D magnetostatic fields*, IEEE Transaction on Magnetics, Vol. 28, No. 2, March 1992, pp. 1056-1059;

[139] Prikler, L., Hoidalen, H., K., *ATPDRAW ver. 3.5 for Windows, Preliminary Release no. 1*, August, 2002;

[140] Răduleţ, R., Timotin, A., Ţugulea, A. *Introducerea parametrilor tranzitorii în studiul circuitelor electrice lineare avînd elemente nefiliforme şi pierderi suplementare*, Revue Roumaine des Sciences Electrotechnique et Énergétiques, Studies and researches in Energetics and Electrical Engineering, Tom 16, No. 4, pp. 857-929, Romanian Academy Publishing House, Bucureşti, 1966;

[141] Răduleţ, R., *Bazele electrotehnicii - probleme*, Vol. I-II, EDP, Bucureşti, 1981;

[142] Ren, Z., Razek, A., *Force calculation by Maxwell stress tensor in 3-D hybrid finite element - boundary integral formulation*, IEEE Transaction on Magnetics, Vol. 26, No. 5, September 1990, pp. 2774-2776;

[143] Ren, Z., *Comparison of different force calculation methods in 3-D finite element modeling*, IEEE Transaction on Magnetics, Vol. 30, No. 5, September 1994, pp. 3471-3474;

[144] Ren, Z., Cendes, Z., *Shell elements for the computation of magnetic forces*, IEEE Transaction on Magnetics, Vol. 37, No. 5, September 2001, pp. 3171-3174;

[145] Sabonnadière, J.C., Coulomb J.L., *La méthode des éléments finis. Du modèle… à la CAO*, Hermes, Paris-Londres-Laussane, 1986;

[146] Shi, Z.W., Rajanathan, C.B., *A new method to improve the accuracy of Maxwell stress based force calculation in computational electromagnetic fields*, Third International Conference on Computation in Electromagnetics, April 10-12, 1996, pp. 241-246;

[147] Silvester, P., Cabayan, H.S., Browne, B.T., *Efficient techniques for finite element analysis of electric machines*, IEEE Transaction on Power Apparatus and Systems, Vol. PAS-92, No. 4, July 1973, pp. 1274-1281;

[148] Smajic, J., Madzarevic, V., Berberovic, S., *Numerical calculation of power transformers equivalent circuit parameters*, International Conference on Electric Power Engineering - PowerTech Budapest '99, August 29 - September 2, 1999, pp. 96;

[149] Spasov, V., *Computation of electromagnetic force by the nodal force method*, 14-th International Symposium on Electrical Apparatus and Technologies - SIELA 2005, Vol. 2, Plovdiv, Bulgaria, June 2-3, 2005, pp. 139-144;

[150] Şora, C., *Bazele electrotehnicii*, EDP, Bucureşti, 1982;

[151] Takahashi, N., Nakata, T., Fujiwara, K., Imai, T., *Investigation of effectiveness of edge elements*, IEEE Transaction on Magnetics, Vol. 28, No. 2, March 1992, pp. 1619-1622;

[152] Takahashi, N., *Investigation of a model to verify software for 3-D static force calculation*, IEEE Transaction on Magnetics, Vol. 30, No. 5, September 1994, pp. 3483-3486;

[166] Yatchev, I., *Modélisation numérique par la méthode des éléments finis*, Seminar, Universitatea din Craiova, 2002;

[153] Takahashi, N., Nakata, T., Morishije, H, *Summary of results for Problem 20* (*3D static force problem*), The International Journal for Computation and Mathematics in Electrical and Electronic Engineering - COMPEL, Vol. 14, No. 2&3, 1995, pp. 57-75, ISSN: 0332-1649;

[154] Tärnhuvud, T., Reichert, K., *Accuracy problems of force and torque calculation in FE-systems*, IEEE Transaction on Magnetics, Vol. 24, No. 1, January 1988, pp. 443-446;

[155] Tihomirov, P.M., *Расчет трансформаторов*, Энергоатомиздат, Москва, 1986;

[156] Timotin, A., Hortopan, V., Ifrim, A., Preda, M., *Lecţii de bazele electrotehnicii*, EDP, Bucureşti, 1970;

[157] Tomczuk, B., Zakrzewski, K., Koteraz, D., *Magnetic field and short-circuit reactance calculation of the 3-phase transformer with symmetrical amorphous core*, 11-th International Symposium on Electromagnetic fields in Electrical Engineering - ISEF 2003, Maribor, Slovenia, September 18-20, 2003, pp. 227-230;

[158] Tsili, M.A., Kladas, A.G., Georgilakis, P.S., Souflaris, A.T., Pitsilis, C.P., Bakopoulos, J.A., Paparigas, D.G., *Hybrid numerical techniques for power transformer modeling: a comparative analysis validated by measurements*, IEEE Transaction on Magnetics, Vol. 40, No. 2, March 2004, pp. 842-845;

[159] Tsili, M.A., Kladas, A.G., Georgilakis, P.S., Souflaris, A.T., Paparigas, D.G., *Geometry optimization of magnetic shunts in power transformers based on a particular hybrid finite-element boundary-element model and sensitivity analysis*, IEEE Transaction on Magnetics, Vol. 41, No. 5, May 2005, pp. 1777-1780;

[160] Tuşaliu, P., Georgescu, D., Matei, D., Chelaru, R., Ivanov, V., Dolan, A., *About modeling of overvoltages in power systems at the transients due to switching operations of multiple capacitor banks*, Scientific works of National Symposium of Electrical Engineering - ELECTRO '99, Vol. I, pp. 153-156, Craiova, Romania, August 27-28, 1999;

[161] Ţugulea, A., *Regimul tranzitoriu al cîmpului electromagnetic inductiv într-un sistem de bare conductoare masive. Parametrii tranzitorii*, Studies and researches in Energetics and Electrical Engineering, Tom 22, No. 1, pp. 67-93, Publishing House Academiei RSR, Bucureşti, 1972;

[162] Webb, F.J., Forghani, B., *A single scalar potential method for 3-D magnetostatics using edge elements*, IEEE Transaction on Magnetics, Vol. 25, No. 5, September 1989, pp. 4126-4128;

[163] Webb, F.J., *Edge elements and what they can do for you*, IEEE Transaction on Magnetics, Vol. 29, No. 2, March 1993, pp. 1460-1465;

[164] Webb, J.P., *An estimator for force errors in finite-element analysis*, IEEE Transaction on Magnetics, Vol. 39, No. 3, May 2003, pp. 1428-1431;

[165] Wignall, A.N., Gilbert, A.J., Yang, S.J., *Calculation of forces on magnetised ferrous cores*, IEEE Transaction on Magnetics, Vol. 24, No. 1, January 1988, pp. 459-462;

[166] Yatchev, I., *Modélisation numérique par la méthode des éléments finis*, Seminar, University of Craiova, 2002;

[167] Yu, H.T., Ho, S.L., Hu, M.Q., Wong, H.C., *Edge-based FEM-BEM for Wide-Band electromagnetic computation*, IEEE Transaction on Magnetics, Vol. 42, No. 4, April 2006, pp. 771-774;

[168] Zienkiewicz, O., Liness, J., *Three magnetic field determination using a scalar potential - A finite element solution*, IEEE Transaction on Magnetics, Vol. MAG-13, No. 5, September 1977, pp. 1649-1656;

[169] Zlatkov, Z., Yatchev, I., Hinov, K., Resano, F., *Static force characteristics of a linear DC actuator using 3D FEM and experiment electromagnet*, International PhD Seminar - Numerical Field Computation and Optimization in Electrical Engineering, Ohrid, Macedonia, September 20-25, 2005, pp. 207-211;

[170] http://www.acad.ro;

[171] http://www.ansys.com/;

[172] http://www.cedrat.com/;

[173] http://www.eeug.org;

[174] http://www.emtp.org/;

[175] http://femm.foster-miller.net;

[176] http://www.lua.org/;

[177] http://www.ocsimize.com/fr/quickfield.htm;

[178] http://www.ptc.com/;

[179] http://www.quickfield.com/.

CURRICULUM VITAE

Full name: **DOLAN Alin-Iulian**

Nationality: Romanian
Date of birth, place: July 1-st, 1971, Craiova, ROMÂNIA
Marital status: Single
Home address: Dr. Victor Papillian Str., No. 1, Bl. A3, Appt. 20 CRAIOVA, 200323, DOLJ, ROMÂNIA

Personal phone: + 40 351 426 259 (home)
+ 40 721 902 301 (mobil)

E-mail: adolan@elth.ucv.ro, alin_dolan@yahoo.com

Profession: Engineer, electrical domain
Place of work: University of Craiova, Electrical Engineering Faculty, ROMANIA
Function: Lecturer
Professional address: Electrical Engineering Faculty, Decebal Bd., No. 107, CRAIOVA, 200440, DOLJ, ROMANIA
Tel. / Fax: + 40 251 436 447
Office phone: + 40 251 435 724 / 127

Studies

Type of diploma	Institution	Year
Certificate of linguistic training General French (378 hours) - level 7/12, level B1 Scientific and Technical French (108 hours)	French Institute of Sofia	2005
Certificate of Teachers Forming Department	University of Craiova	2002
Master Degree in Electrical Engineering, Ecological Technologies Specialization	Electrical Engineering Faculty, University of Craiova	1996
Degree in Electrical Engineering, General Electrical Engineering Specialization	Electrical Engineering Faculty, University of Craiova	1995
Baccalaureate Diploma in Electronics	High School Mathematics and Physics Nicolae Bălcescu, Craiova	1990

Professional experience

Function	Institution	Period
Lecturer	Electrical Engineering Faculty, University of Craiova	23.02.2009 - present
University assistant	Electrical Engineering Faculty, University of Craiova	25.02.2002 - 22.02.2009
Junior assistant	Electrical Engineering Faculty, University of Craiova	01.03.1999 - 24.02.2002
Teacher	Pop Service Electronic HQ, Craiova	01.04.1998 - 31.05.1998

Abroad stages

Stage type	Institution	Period
PhD. Training - University Agency for Francophonie (AUF) Program no. 6 - Scientific and university mobility	International Engineering Doctoral School, Francophone Department, Technical University of Sofia Scientific coordinator: Prof. Ivan YATCHEV	31.03.2007 - 01.08.2007
	National Polytechnic Institute of Grenoble, Electrical Engineering Laboratory of Grenoble Scientific coordinators: Prof. Gérard MEUNIER Prof. Albert FOGGIA	02.10.2006 - 30.03.2007
PhD. Training - University Agency for Francophonie (AUF) Program no. 5 - Scientific and institutional reinforcement of universities	International Doctoral School in Engineering, Francophone Department, Technical University of Sofia, Regional Network Engineering for Development (RENED) Scientific coordinator: Prof. Ivan YATCHEV	02.08.2007 - 01.09.2007
		26.07.2006 - 31.08.2006
		01.11.2004 - 22.12.2005
Linguistic training - French Embassy in Bulgaria, Cooperation and Cultural Center	French Institute of Sofia	01.10.2004 - 22.12.2005
		26.07.2004 - 31.08.2004

Scientific experience

- 5 research contracts
- 15 scientific papers

Informatics competences

- MICROSOFT OFFICE, TURBOPASCAL, FORTRAN, C++, MATHCAD, MATLAB, QUICKFIELD, FEMM (LUASCRIPT), ANSYS (APDL), ATP-EMTP, FLUX

Teaching fields

- Electrical apparatus - applications
- Electrical equipments - applications
- CAD of Electrical Equipments - applications
- High Voltage Engineering - applications
- Theoretical Electrical Engineering - applications
- Computer programming and programming languages - applications
- Statistical Models and Reliability - course
- Reliability - course

Foreign languages:

- French: read, speak, write
- English: read, speak, write

13.11.2009 Signature: